

Nonlinear Causal Discovery via Kernel Anchor Regression

Wenqi Shi¹Wenkai Xu²¹Department of Industrial Engineering, Tsinghua University²Department of Statistics, University of Oxford

Abstract

Learning causal relationships is a fundamental problem in science. Anchor regression has been developed to address this problem for a large class of causal graphical models, though the relationships between the variables are assumed to be linear. In this work, we tackle the nonlinear setting by proposing kernel anchor regression (KAR). Beyond the natural formulation using a classic two-stage least square estimator, we also study an improved variant that involves nonparametric regression in three separate stages. We provide convergence results for the proposed KAR estimators and the identifiability conditions for KAR to learn the nonlinear structural equation models (SEM). Experimental results demonstrate the superior performances of the proposed KAR estimators over existing baselines.

1 Introduction

Causal relationships are concerned with consequences of actions or decisions; thus, understanding these relationships can be the key ingredient in many scientific studies. For instance, medical practitioners need to know whether a treatment is effective to the target disease in clinical trials; econometricians ask whether a particular purchasing behaviour drives a change in Consumer Price Index (CPI); epidemiologists want to understand whether a government intervention policy has a positive effect on the pandemic. While the goal of revealing causal effects remains the same, the focus in causal relationships can differ by applications. To describe different aspects of the causal notion and design statistical procedures for inferring causal effects, various frameworks have been developed including Rubin’s potential outcome framework [Rubin, 2004, 2005], counterfactual distributions [Chernozhukov et al., 2013] and Pearl’s causal graphical models [Pearl et al., 2000, 2016]. A succinct yet comprehensive introduction can be found in Peters et al. [2017].

Causality has also been an evolving field in machine learning community and machine learning techniques have been considered to improve the statistical procedures for causal discovery. In particular, nonparametric independence [Gretton et al., 2005] and conditional independence [Fukumizu et al., 2007] measures have been exploited to infer causal graphical models [Colombo

et al., 2012; Mooij et al., 2009], especially with additive noise [Hoyer et al., 2008; Peters et al., 2014]. Independent Component Analysis (ICA) methods [Hyvärinen, 2013; Hyvarinen and Morioka, 2017] have been employed to identify causal relationship in both linear [Hyvärinen et al., 2010; Shimizu et al., 2006, 2011] and non-linear settings [Monti et al., 2020; Khemakhem et al., 2021]. Score matching [Hyvärinen and Dayan, 2005] has also been considered [Rolland et al., 2022] for non-linear causal discovery. Moreover, kernel methods, that utilize rich representation of reproducing kernel Hilbert space (RKHS), have been applied to tackle nonparametric estimation [Muandet et al., 2021; Singh et al., 2019] and regression [Singh et al., 2019; Zhu et al., 2022] problems with causal implications. Deep neural networks have also been attempted for learning treatment effect [Johansson et al., 2020; Kallus, 2020; Louizos et al., 2017] or useful causal representations [Besserve et al., 2019; Schölkopf et al., 2021; Xu et al., 2020, 2021].

Recently, an elegant and statistically robust approach formulates causality as an invariant risk minimization (IRM), see for example [Bühlmann, 2018; Peters et al., 2016]. The causal structure is thought to be invariant across the environment and robust under intervention. The IRM learning procedure [Arjovsky et al., 2019] on the observational data is then formulated as a regularised empirical risk minimization (ERM) to achieve both in-distribution performance and out-of-distribution generalization. In particular, anchor regression [Rothenhäusler et al., 2018] has been developed under the IRM framework to tackle a very general class of causal graphical models with the confounders being partly (but not fully) observed. By choosing different regularisation parameter, anchor regression is able to unify the ordinary least square (OLS) regression, partialling out (PA) regression, and instrumental variable (IV) regression. While existing works [Oberst et al., 2021; Rothenhäusler et al., 2018] mostly considered linear cases, we explore the non-linear setting for anchor regression [Kook et al., 2022]. Specifically, we consider the nonparametric estimation to tackle non-linear features via RKHS functions.

The paper is structured as follows. In Section 2, we review useful concepts including instrumental variable (IV), anchor regression (AR), and reproducing kernel Hilbert space (RKHS). Then we develop two versions of kernel anchor regression (KAR) estimators in Section 3. Theoretical analysis on the estimators and the causal interpretation with nonlinear SEM are provided in Section 4. Experimental results for synthetic data and real-world applications are shown in Section 5 followed by concluding discussion and future directions in Section 6. The code for the experiments is available in at <https://github.com/Swq118/Kernel-Anchor-Regression>.

2 Background

Directed Acyclic Graph (DAG) is a power class of graphical model for characterising conditional dependency structures and has been widely used for probabilistic modelling such as hidden Markov models [Rabiner and Juang, 1986], latent variable models [Bishop, 1998] and topic models [Blei, 2012]. By enforcing certain Markov and faithfulness assumptions [Peters et al.,

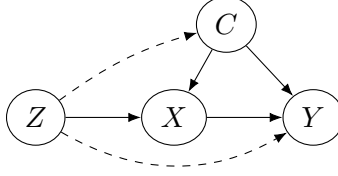


Figure 1: IV regression (solid lines only) and anchor regression (with dashed lines).

2011], as well as noise structures [Hoyer et al., 2008], DAG models the causal relationships [Glymour et al., 2019; Spirtes et al., 2013] and the learning procedures have been developed [Colombo et al., 2012; Spirtes et al., 2000; Zhang et al., 2018].

From Instrumental Variable to Anchor Regression

Instrumental variable (IV) has been developed to incorporate endogenous explanatory variables in econometrics [Bowden and Turkington, 1990] and then applied for estimating causal effect [Angrist et al., 1996]. Consider the linear regression problem $Y = X\beta + \epsilon$. OLS assumes independence between noise ϵ and explanatory X (the exogenous variable) and β is estimated via minimizing

$$\beta^{OLS} = \arg \min_{\beta} \mathbb{E}_{train}[\|Y - X\beta\|^2]. \quad (1)$$

The IV setting assumes explicit dependency between X and ϵ via instrumental variable Z , i.e. $X = Z\theta + \varepsilon$ where $Z \perp \varepsilon$. The two-stage least squares (2SLS) procedure, widely used in economics, tackles the linear IV estimation by first regressing Z over X to get conditional means $\bar{X}(z) := \mathbb{E}[X|Z = z]$ and secondly regressing outputs Y on these conditional means¹. This corresponds to minimizing the projected least square objective,

$$\beta^{IV} = \arg \min_{\beta} \mathbb{E}_{train}[\|P_Z(Y - X\beta)\|^2]. \quad (2)$$

P_Z denotes the projection to Z where $P_{Z=z}(X) = \mathbb{E}[X|Z = z] = \bar{X}(z)$. 2SLS works well when the underlying assumptions hold. The corresponding DAG is shown in Figure 1 with only solid lines. In practice, the relation between Y and X may not be linear, nor may be the relation between X and Z . Nonlinear IV has been explored [Bennett et al., 2019; Centorrino et al., 2019; Hartford et al., 2017; Singh et al., 2019; Xu et al., 2020; Zhu et al., 2022].

However, Y 's dependency on Z may not be solely through X , i.e. as the dashed lines from Z to Y in Figure 1 indicate, Y may depend on Z directly, even though the strength of such dependency may remain unknown. The latent confounder C may not be independent of Z , as

¹For the second stage, by writing $Y = X\beta + \epsilon = \underbrace{Z\theta}_{\mathbb{E}[X|Z]} + (\varepsilon\beta + \epsilon)$, then the regressor is independent of noise and the OLS estimator can then apply.

indicated by dashed line from Z to C in Figure 1. Incorporating such dependency structures tackles a much more general class of DAG, e.g. IV is a special case. To estimate β , anchor regression has been proposed [Rothenhäusler et al., 2018] that effectively combines Equation (1) and Equation (2). For chosen regularization parameter γ and identity operator $Id(Z) := Z$,

$$\beta^\gamma = \arg \min_{\beta} \mathbb{E}_{train} [\| (Id - P_Z)(Y - X\beta) \|^2] \quad (3)$$

$$+ \gamma \mathbb{E}_{train} [\| P_Z(Y - X\beta) \|^2]. \quad (4)$$

Here, $\gamma \geq 0$ can be thought of the level of dependencies of Y from Z variable². By setting different γ values, anchor regression resembles classical settings, i.e. $\gamma = 1$ corresponds to OLS, $\beta^1 = \beta^{OLS}$; $\gamma \rightarrow \infty$ corresponds to IV, $\beta^{\infty} := \lim_{\gamma \rightarrow \infty} \beta^\gamma = \beta^{IV}$; $\gamma = 0$ corresponds to the "partialling out" setting where only residuals between regression of Z to X and Y are of interest.

Kernel-based Methods

Kernel methods employ functions in RKHS to tackle various statistical and machine learning tasks with nonlinear features [Hofmann et al., 2008], e.g. kernel ridge regression, support vector machine [Scholkopf and Smola, 2018; Steinwart and Christmann, 2008], etc. Functions in RKHS have also been developed to represent and characterize distributions, via kernel mean embedding [Muandet et al., 2017]. For probability measure p , and kernel k associated with RKHS \mathcal{H} , the mean embedding $\mu_p := \int k(x, \cdot) dp(x) \in \mathcal{H}$. This notion has been widely used to compare distributions, e.g. via maximum-mean-discrepancy (MMD) [Gretton et al., 2012]. With p being a conditional distribution, conditional mean embedding [Song et al., 2009] has also been considered for learning and regression problems. Various techniques have also been developed to formulate and learn operators to manipulate conditional mean embeddings [Fukumizu et al., 2007; Grünewälder et al., 2012]. With the rich representation of nonlinear features, RKHS functions are also applicable of learning distribution directly via distribution regression [Szabó et al., 2015, 2016].

3 Kernel Anchor Regression

To capture the non-linear features in the DAG, we kernelize the anchor regression framework by utilizing the rich feature representation of RKHS functions. The kernelizing procedure is inspired from kernel instrumental variable (KIV) [Singh et al., 2019] where the operators are learned for conditional mean embedding in two separate regression stages. The DAG representation is illustrated in Figure 2.

Let $k_{\mathcal{X}} : \mathcal{X} \times \mathcal{X} \rightarrow \mathbb{R}$, $k_{\mathcal{Z}} : \mathcal{Z} \times \mathcal{Z} \rightarrow \mathbb{R}$ be measurable positive definite kernels corresponding to RKHS $\mathcal{H}_{\mathcal{X}}$ and $\mathcal{H}_{\mathcal{Z}}$. Denote the feature maps $\psi : \mathcal{X} \rightarrow \mathcal{H}_{\mathcal{X}}$, $x \rightarrow k_{\mathcal{X}}(x, \cdot)$ and $\phi : \mathcal{Z} \rightarrow$

²The smaller γ value dashed line, the stronger the dependency, i.e. the more solid dashed line from Z to Y .

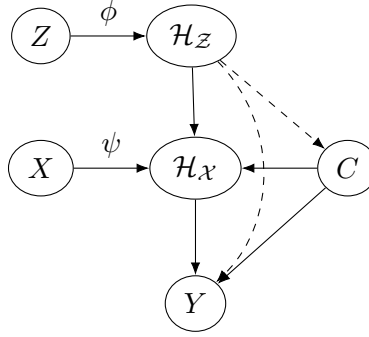


Figure 2: DAG representation for kernel anchor regression.

$\mathcal{H}_Z, z \rightarrow k_Z(z, \cdot)$. Let $P_{\phi(Z)}$ and Id denote the L_2 -projection on the linear span from the components of $\phi(Z)$ and the identity operator, respectively. Denote $H : \mathcal{H}_X \rightarrow \mathcal{Y}$ as the conditional operator we aim to learn. Then for $\gamma \geq 0$, define the population-level kernel anchor regression operator H^γ as

$$H^\gamma = \arg \min_H \mathbb{E}[\|(Id - P_{\phi(Z)})(Y - H\psi(X))\|^2] + \gamma \mathbb{E}[\|P_{\phi(Z)}(Y - H\psi(X))\|^2]. \quad (5)$$

To unravel $P_{\phi(Z)}$, both IV and AR estimators applied the two-stage procedure, where the first stage is to estimate the projection operator $P_{\phi(Z)}$ and the second stage is to perform the projection adjusted regression.

3.1 Projection Stage

The projection stage aims to tackle $P_{\phi(Z)}$ by transforming the problem of learning $P_{\phi(Z)}\psi(X)$ and $P_{\phi(Z)}Y$ into two separate kernel ridge regressions. Let operators $E_X : \mathcal{H}_Z \rightarrow \mathcal{H}_X$ and $E_Y : \mathcal{H}_Z \rightarrow \mathcal{Y}$ be the projections to learn³; $\alpha_1, \alpha_2 > 0$ be regularization parameters. The objectives regularized by Hilbert-Schmidt (HS) norm are

$$\mathcal{E}_{\alpha_1}(E_X) = \mathbb{E}\|\psi(X) - E_X\phi(Z)\|_{\mathcal{H}_X}^2 + \alpha_1\|E_X\|_{HS}^2, \quad (6)$$

$$\mathcal{E}_{\alpha_2}(E_Y) = \mathbb{E}\|Y - E_Y\phi(Z)\|_{\mathcal{Y}}^2 + \alpha_2\|E_Y\|_{HS}^2. \quad (7)$$

Denote the optimal operators for the population risks as $E_{\alpha_1, X}^p = \arg \min_{E_X} \mathcal{E}_{\alpha_1}(E_X)$, and $E_{\alpha_2, Y}^p = \arg \min_{E_Y} \mathcal{E}_{\alpha_2}(E_Y)$. We then consider two variants of empirical risks and their corresponding estimations.

³We note that due to the explicit dependency from Z to Y , $P_{\phi(Z)}Y$ needs to be treated separately from $P_{\phi(Z)}\psi(X)$. This is different from the IV setting where $P_{\phi(Z)}Y = Y$ as the edge from Z to Y in the DAG is absent.

3.1.1 Disjoint sample sets projection

Firstly, we treat two ridge regression in Equation (6) and Equation (7) independently, by using two *disjoint* sets of samples $\mathbb{S}_1 = \{(x_i, z_i)\}_{i \in [n_1]}$ and $\mathbb{S}_2 = \{(y_j, z_j)\}_{j \in [n_2]}$. The empirical forms for Equation (6) and Equation (7) are

$$\frac{1}{n_1} \sum_{i \in [n_1]} \|\psi(x_i) - E_X \phi(z_i)\|_{\mathcal{H}_X}^2 + \alpha_1 \|E_X\|_{HS}^2, \quad (8)$$

$$\frac{1}{n_2} \sum_{j \in [n_2]} \|y_j - E_Y \phi(z_j)\|_Y^2 + \alpha_2 \|E_Y\|_{HS}^2. \quad (9)$$

Denote by $\Phi_{1,Z} = (\phi(z_1), \dots, \phi(z_{n_1})), \{z_i\}_{i \in [n_1]} \subset \mathbb{S}_1$; $\Phi_{2,Z} = (\phi(z_1), \dots, \phi(z_{n_2})), \{z_j\}_{j \in [n_2]} \subset \mathbb{S}_2$; their corresponding gram matrices $K_{1,ZZ} = \Phi_{1,Z}^\top \Phi_{1,Z} \in \mathbb{R}^{n_1 \times n_1}$ and $K_{2,ZZ} = \Phi_{2,Z}^\top \Phi_{2,Z} \in \mathbb{R}^{n_2 \times n_2}$. Denote $\Psi_{1,X} = (\psi(x_1), \dots, \psi(x_{n_1})), \{x_i\}_{i \in [n_1]} \subset \mathbb{S}_1$ and $Y_2 = (y_1, \dots, y_{n_2}), \{y_j\}_{j \in [n_2]} \subset \mathbb{S}_2$. By the standard regression formula, the optimal operators to minimize Equation (8) and Equation (9) are

$$E_{\alpha_1, X}^{n_1} = \Psi_{1,X} (K_{1,ZZ} + n_1 \alpha_1 I)^{-1} \Phi_{1,Z}^\top, \quad (10)$$

$$E_{\alpha_2, Y}^{n_2} = Y_2 (K_{2,ZZ} + n_2 \alpha_2 I)^{-1} \Phi_{2,Z}^\top, \quad (11)$$

where the superscripts n_1, n_2 explicitly reveal sample sizes. We note that the projections $P_{\phi(Z)}$ are estimated differently for $P_{\phi(Z)}\psi(X)$ and $P_{\phi(Z)}Y$, through $(K_{1,ZZ} + n_1 \alpha_1 I)^{-1}$ and $(K_{2,ZZ} + n_2 \alpha_2 I)^{-1}$, respectively. $K_{1,ZZ}$ and $K_{2,ZZ}$ are independent due to the use of disjoint i.i.d. sample sets of Z .

3.1.2 Joint sample set projection

On the other hand, we can also consider the projection analogous to [Rothenhäusler et al. \[2018\]](#) where we jointly consider the samples used for both projections, i.e. projecting onto the same $\phi(Z)$ subspace. Setting $n = n_1 + n_2$ and $\alpha_1 = \alpha_2 = \alpha$, we consider the joint sample set $\mathbb{S} = \{(x_i, y_i, z_i)\}_{i \in [n]}$ and the empirical risks

$$\frac{1}{n} \sum_{i \in [n]} \|\psi(x_i) - E_X \phi(z_i)\|_{\mathcal{H}_X}^2 + \alpha \|E_X\|_{HS}^2, \quad (12)$$

$$\frac{1}{n} \sum_{i \in [n]} \|y_i - E_Y \phi(z_i)\|_Y^2 + \alpha \|E_Y\|_{HS}^2. \quad (13)$$

Denote $K_{ZZ} \in \mathbb{R}^{n \times n}$ as the gram matrix from $\{z_i\}_{i \in [n]} \subset \mathbb{S}$; $\Phi_Z = (\phi(z_1), \dots, \phi(z_n)), \{z_i\}_{i \in [n]} \subset \mathbb{S}$; $\Psi_X = (\psi(x_1), \dots, \psi(x_n)), \{x_i\}_{i \in [n]} \subset \mathbb{S}$ and $Y = (y_1, \dots, y_n), y_i \in \mathbb{S}$. Then we have

$$E_{\alpha, X}^n = \Psi_X (K_{ZZ} + n \alpha I)^{-1} \Phi_Z^\top, \quad (14)$$

$$E_{\alpha, Y}^n = Y^\top (K_{ZZ} + n \alpha I)^{-1} \Phi_Z^\top. \quad (15)$$

By setting the same level of regularisation, we can see that the $P_{\phi(Z)}$ projection, through $(K_{ZZ} + n\alpha I)^{-1}$, are the same for $P_{\phi(Z)}\psi(X)$ and $P_{\phi(Z)}Y$.

3.2 Regression Stage

With the learned projections $P_{\phi(Z)}\psi(X)$ and $P_{\phi(Z)}Y$, we can now tackle the overall objective in Equation (5).

Denote $\mathcal{E}(E_X)$ and $\mathcal{E}(E_Y)$ as the unregularized version of Equation (6) and Equation (7); E_X^p and E_Y^p their corresponding optimal operators, respectively. For given γ , define the transformed input and output as

$$\psi_\gamma(X) = \psi(X) - E_X^p\phi(Z) + \sqrt{\gamma}E_X^p\phi(Z) \in \mathcal{H}_X, \quad (16)$$

$$Y_\gamma = Y - E_Y^p\phi(Z) + \sqrt{\gamma}E_Y^p\phi(Z) \in \mathcal{Y}. \quad (17)$$

Proposition 1 (Equivalence). Let $H : \mathcal{H}_X \rightarrow \mathcal{Y}$, and consider the regression of transformed output in Equation (17) on transformed input in Equation (16)

$$\mathcal{E}^\gamma(H) = \mathbb{E}_{(Z,X,Y)} \|Y_\gamma - H\psi_\gamma(X)\|_{\mathcal{Y}}^2. \quad (18)$$

The solution to Equation (18) is equivalent to the KAR estimator in Equation (5), i.e. $H^\gamma = \arg \min_H \mathcal{E}^\gamma(H)$.

The proof is by expanding the projection operator E_X^p and E_Y^p , which is similar to the linear case in [Rothenhäusler et al. \[2018\]](#).

With regularization parameter $\xi \geq 0$, Equation (18) has the kernel ridge regression form defined as

$$\mathcal{E}_\xi^\gamma(H) = \mathbb{E}_{(Z,X,Y)} \|Y_\gamma - H\psi_\gamma(X)\|_{\mathcal{Y}}^2 + \xi \|H\|_{HS}^2. \quad (19)$$

The regression stage is formulated regardless how the projections are estimated in Section 3.1. For the empirical version, we consider the estimated operators $\widehat{E}_X \in \{E_{\alpha_1, X}^{m_1}, E_{\alpha, X}^n\}$ and $\widehat{E}_Y \in \{E_{\alpha_2, Y}^{n_2}, E_{\alpha, Y}^n\}$. With samples $\mathbb{S}^m = \{(x_l, y_l, z_l)\}_{l \in [m]}$, we compute the transformed inputs and outputs as

$$\widehat{\psi}_{\gamma, l}(x) = \psi(x_l) + (\sqrt{\gamma} - 1)\widehat{E}_X\phi(z_l) \in \mathcal{H}_X,$$

$$\widehat{y}_{\gamma, l} = y_l + (\sqrt{\gamma} - 1)\widehat{E}_Y\phi(z_l) \in \mathcal{Y}.$$

The empirical risk has the form

$$\widehat{\mathcal{E}}_\xi^{\gamma, m}(H) = \frac{1}{m} \sum_{l \in [m]} \|\widehat{y}_{\gamma, l} - H\widehat{\psi}_{\gamma, l}(x)\|_{\mathcal{Y}}^2 + \xi \|H\|_{HS}^2, \quad (20)$$

$$\widehat{H}_\xi^{\gamma,m} = \arg \min \widehat{\mathcal{E}}_\xi^{\gamma,m}(H).$$

Denote $\widehat{\Psi}_\gamma = (\widehat{\psi}_{\gamma,1}(x), \dots, \widehat{\psi}_{\gamma,m}(x))$ and its gram matrix $K_{\widehat{\Psi}_\gamma \widehat{\Psi}_\gamma} = \widehat{\Psi}_\gamma^\top \widehat{\Psi}_\gamma \in \mathbb{R}^{m \times m}$; $\widehat{Y}_\gamma = (\widehat{y}_{\gamma,1}, \dots, \widehat{y}_{\gamma,m})$. Again, by standard regression formula,

$$\widehat{H}_\xi^{\gamma,m} = \widehat{Y}_\gamma (K_{\widehat{\Psi}_\gamma \widehat{\Psi}_\gamma} + m\xi I)^{-1} \widehat{\Psi}_\gamma^\top. \quad (21)$$

3.3 KAR Estimator

Given observational data of size N , $\{(x_i, y_i, z_i)\}_{i \in [N]}$, the KAR procedure can be performed in two ways based on the two variants in the projection stage.

Three-stage KAR To apply the disjoint sample sets projection in Section 3.1.1, we *randomly* split the data set of size N into three disjoint sets of sample size n_1, n_2, m where $N = n_1 + n_2 + m$ and re-index them from $\{1 : N\}$. The first two sets of data $\{(x_i, z_i)\}_{i \in \{1:n_1\}}$ and $\{(y_j, z_j)\}_{j \in \{n_1+1:n_1+n_2\}}$ are used for learning the projection operators in Equation (10) and Equation (11). We note that samples $\{y_i\}_{i \in \{1:n_1\}}$ and $\{x_j\}_{j \in \{n_1+1:n_1+n_2\}}$ are not used. The third set $\{(x_l, y_l, z_l)\}_{l \in \{n_1+n_2+1:N\}}$ is used for regression stage to learn $\widehat{H}_\xi^{\gamma,m}$ in Equation (21). This procedure, termed **KAR**, includes solving three different regression problems, which is different from the two-stage settings used in linear anchor regression [Rothenhäusler et al., 2018].

Two-stage KAR For the joint sample set projection in Section 3.1.2, we only split the data of size N into two disjoint sets *randomly* of size n and m where $N = n + m$ and re-index them such that $\{(x_i, y_i, z_i)\}_{i \in \{1:n\}}$ and $\{(x_l, y_l, z_l)\}_{l \in \{n+1:N\}}$. The first set is then grouped into $\{(x_i, z_i)\}_{i \in \{1:n\}}$ and $\{(y_i, z_i)\}_{j \in \{1:n\}}$ to learn the projection operators in Equation (10) and Equation (11). In this manner, $\{z_i\}_{i \in \{1:n\}}$ are used twice. The second set $\{(x_l, y_l, z_l)\}_{l \in \{n+1:N\}}$ is used for regression stage to learn $\widehat{H}_\xi^{\gamma,m}$ in Equation (21), which is the same as the three-stage procedure above. This procedure, termed **KAR.2**, replicates the 2SLS used in KIV [Singh et al., 2019] and linear anchor regression [Rothenhäusler et al., 2018].

4 Analysis of KAR Estimators

4.1 Consistency

In this section, we first focus on the three-stage KAR procedure with disjoint sample sets for projection in Section 3.1.1. The closed form solutions and convergence rates of the estimators are extended from the analysis of 2SLS in KIV [Singh et al., 2019]. We follow the integral operator notations in Singh et al. [2019]. Define the projection stage operators as

$$\begin{aligned} S_1^* &: \mathcal{H}_Z \rightarrow L^2(\mathcal{Z}, \rho_Z), \quad l \rightarrow \langle l, \phi(\cdot) \rangle_{\mathcal{H}_Z}, \\ S_1 &: L^2(\mathcal{Z}, \rho_Z) \rightarrow \mathcal{H}_Z, \quad \tilde{l} \rightarrow \int \phi(z) \tilde{l}(z) d\rho_Z(z), \end{aligned}$$

where ρ denotes the joint distribution of (Z, X, Y) . $L^2(\mathcal{Z}, \rho_Z)$ denotes the space of square integrable functions from \mathcal{Z} to \mathcal{Y} with respect to measure ρ_Z , where ρ_Z is the restriction of ρ to \mathcal{Z} . $T_1 = T_2 = S_1 \circ S_1^*$ are then uncentered covariance operators. We define the power of operator T_1 with respect to its eigendecomposition. Let $\mathcal{H}_\Gamma = \mathcal{H}_X \otimes \mathcal{H}_Z$, $\mathcal{H}_\Theta = \mathcal{Y} \otimes \mathcal{H}_Z$ and $\mathcal{H}_\Omega = \mathcal{Y} \otimes \mathcal{H}_X$ be the relevant tensor product spaces for the operators.

Condition 1. (i) \mathcal{X} and \mathcal{Z} are Polish, i.e. separable and completely metrizable topological spaces. (ii) k_X and k_Z are continuous and bounded: $\sup_{x \in \mathcal{X}} \|\psi(x)\|_{\mathcal{H}_X} \leq Q_1$, $\sup_{z \in \mathcal{Z}} \|\phi(z)\|_{\mathcal{H}_Z} \leq \kappa$. (iii) ψ and ϕ are measurable. (iv) k_X is characteristic. (v) $E_X^p \in \mathcal{H}_\Gamma$ s.t. $\mathcal{E}(E_X^p) = \inf_{E_X \in \mathcal{H}_\Gamma} \mathcal{E}(E_X)$. (vi) Fix $\zeta_1 < \infty$. For $c_1 \in (1, 2]$, define the prior $\mathcal{P}(\zeta_1, c_1)$ as the set of probability distributions ρ on $\mathcal{X} \times \mathcal{Z}$ s.t. $\exists G_1 \in \mathcal{H}_\Gamma$ s.t. $E_X^p = T_1^{(c_1-1)/2} \circ G_1$ and $\|G_1\|_{\mathcal{H}_\Gamma}^2 \leq \zeta_1$.

Condition 1 is adapted from Singh et al. [2019] to bound the approximation error of the regularized estimator $E_{\alpha_1, X}^{n_1}$. Parameter c_1 suggests the smoothness of conditional operator $E_{\alpha_1, X}^{n_1}$. A larger c_1 corresponds to a smoother operator.

Lemma 1. $\forall \alpha_1 > 0$, the solution $E_{\alpha_1, X}^{n_1}$ of the regularized empirical objective in Equation (8) exists and is unique. With $\mathbf{T}_1 = \frac{1}{n_1} \sum_{i=1}^{n_1} \phi(z_i) \otimes \phi(z_i)$ and $\mathbf{g}_1 = \frac{1}{n_1} \sum_{i=1}^{n_1} \phi(z_i) \otimes \psi(x_i)$, the estimator in Equation (10) has the form $E_{\alpha_1, X}^{n_1} = (\mathbf{T}_1 + \alpha_1)^{-1} \circ \mathbf{g}_1$.

Under Condition 1 and $\alpha_1 = n_1^{-1/(c_1+1)}$, we have:

$$\|E_{\alpha_1, X}^{n_1} - E_X^p\|_{\mathcal{H}_\Gamma} = O_p(n_1^{-\frac{c_1-1}{2(c_1+1)}}).$$

Lemma 1 follows from Singh et al. [2019], and shows that the efficient rate of α_1 is $n_1^{-1/(1+c_1)}$. Note that the convergence rate of $E_{\alpha_1, X}^{n_1}$ is calibrated by c_1 , which measures the smoothness of the conditional expectation operator E_X .

For the disjoint set projection in Section 3.1.1, the closed form solution and convergence rate for learning $P_{\phi(Z)}Y$ estimator is similar to that of learning $P_{\phi(Z)}\psi(X)$ due to the independent estimation procedure and further requires the following conditions.

Condition 2. (i) \mathcal{Y} is a Polish space. (ii) Y is bounded: $\sup_{y \in \mathcal{Y}} \|y\|_{\mathcal{Y}} \leq Q_2$. (iii) $E_Y^p \in \mathcal{H}_\Theta$ s.t. $\mathcal{E}(E_Y^p) = \inf_{E_Y \in \mathcal{H}_\Theta} \mathcal{E}(E_Y)$. (iv) Fix $\zeta_2 < \infty$. For $c_2 \in (1, 2]$, define the prior $\mathcal{P}(\zeta_2, c_2)$ as the set of probability distributions ρ on $\mathcal{Y} \times \mathcal{Z}$ s.t. $\exists G_2 \in \mathcal{H}_\Theta$ s.t. $E_Y^p = T_2^{(c_2-1)/2} \circ G_2$ and $\|G_2\|_{\mathcal{H}_\Theta}^2 \leq \zeta_2$.

Lemma 2. $\forall \alpha_2 > 0$, the solution $E_{\alpha_2, Y}^{n_2}$ of the regularized empirical objective in Equation (9) exists and is unique. With $\mathbf{T}_2 = \frac{1}{n_2} \sum_{j=1}^{n_2} \phi(z_j) \otimes \phi(z_j)$ and $\mathbf{g}_2 = \frac{1}{n_2} \sum_{j=1}^{n_2} \phi(z_j)y_j$, the estimator in Equation (10) has the form $E_{\alpha_2, Y}^{n_2} = (\mathbf{T}_2 + \alpha_2)^{-1} \circ \mathbf{g}_2$. Under Condition 1–2 and $\alpha_2 = n_2^{-1/(c_2+1)}$, we have:

$$\|E_{\alpha_2, Y}^{n_2} - E_Y^p\|_{\mathcal{H}_\Theta} = O_p(n_2^{-\frac{c_2-1}{2(c_2+1)}}).$$

Similar to learning projection $P_{\phi(Z)}\psi(X)$, the efficient rate of α_2 is $n_2^{-1/(1+c_2)}$, where c_2 measures the smoothness of the conditional expectation operator E_Y .

Let $L^2(\mathcal{H}_X, \rho_{\mathcal{H}_X})$ denote the space of square integrable functions from \mathcal{H}_X to \mathcal{Y} with respect to measure $\rho_{\mathcal{H}_X}$, where $\rho_{\mathcal{H}_X}$ is the extension of ρ to \mathcal{H}_X . Define the regression stage operator as

$$\begin{aligned} S^* &: \mathcal{H}_\Omega \rightarrow L^2(\mathcal{H}_X, \rho_{\mathcal{H}_X}), \quad H \rightarrow \Omega_{(\cdot)}^* H, \\ S &: L^2(\mathcal{H}_X, \rho_{\mathcal{H}_X}) \rightarrow \mathcal{H}_\Omega, \\ \tilde{H} &\rightarrow \int \Omega_{\psi_\gamma} \circ \tilde{H} \psi_\gamma d\rho_{\mathcal{H}_X}(\psi_\gamma), \end{aligned}$$

where $\Omega_{\psi_\gamma} : \mathcal{Y} \rightarrow \mathcal{H}_\Omega$ defined by $y \rightarrow \Omega(\cdot, \psi_\gamma)y$ is the point evaluator of [Micchelli and Pontil \[2005\]](#). Define $T_{\psi_\gamma} = \Omega_{\psi_\gamma} \circ \Omega_{\psi_\gamma}^*$ and covariance operator $T = S \circ S^*$. Define the power of operator T with respect to its eigendecomposition. Condition 3 below extends hypothesis 7–9 in [Singh et al. \[2019\]](#), and is sufficient to bound the excess error of $\widehat{H}_\xi^{\gamma, m}$ with the error propagated from the estimators in the projection stage.

Condition 3. (i) The $\{\Omega_{\psi_\gamma}\}$ operator family is uniformly bounded in Hilbert-Schmidt norm:

$$\exists B \text{ s.t. } \forall \psi_\gamma, \|\Omega_{\psi_\gamma}\|_{L_2(\mathcal{Y}, \mathcal{H}_\Omega)}^2 = \text{Tr}(\Omega_{\psi_\gamma}^* \circ \Omega_{\psi_\gamma}) \leq B.$$

(ii) The $\{\Omega_{\psi_\gamma}\}$ operator family is Hölder continuous in operator norm: $\exists L > 0, \iota \in (0, 1]$

$$\text{s.t. } \forall \psi_\gamma, \psi'_\gamma, \|\Omega_{\psi_\gamma} - \Omega_{\psi'_\gamma}\|_{L(\mathcal{Y}, \mathcal{H}_\Omega)} \leq L \|\psi_\gamma - \psi'_\gamma\|_{\mathcal{H}_X}^\iota.$$

(iii) $H^\gamma \in \mathcal{H}_\Omega$, then $\mathcal{E}^\gamma(H^\gamma) = \inf_{H \in \mathcal{H}_\Omega} \mathcal{E}^\gamma(H)$.

(iv) Y_γ is bounded, i.e. $\exists C < \infty$ s.t. $\|Y_\gamma\|_{\mathcal{Y}} \leq C$.

(v) Fix $\zeta < \infty$. For given $b_\gamma \in (1, \infty]$ and $c_\gamma \in (1, 2]$, define the prior $\mathcal{P}(\zeta, b_\gamma, c_\gamma)$ as the set of probability distributions ρ on $\mathcal{H}_X \times \mathcal{Y}$ s.t.

(a) range space assumption is satisfied: $\exists G \in \mathcal{H}_\Omega$ s.t. $H^\gamma = T^{\frac{(c_\gamma-1)}{2}} \circ G$ and $\|G\|_{\mathcal{H}_\Omega}^2 \leq \zeta$;

(b) the eigenvalues from spectral decomposition $T = \sum_{k=1}^{\infty} \lambda_k e_k \langle \cdot, e_k \rangle_{\mathcal{H}_\Omega}$, where $\{e_k\}_{k=1}^{\infty}$ is a basis of $\text{Ker}(T)^\perp$, satisfy $\alpha \leq k^{b_\gamma} \lambda_k \leq \beta$ for some $\alpha, \beta > 0$.

We note that all parameters mentioned in Condition 3 depend on γ , though the function representations are not explicit. We set subscript γ especially for parameters b_γ and c_γ to emphasize their dependency on γ . Parameter b_γ measures the decay of eigenvalues of the covariance operator T and specifically, larger b_γ suggests smaller effective input dimension. A larger c_γ corresponds to a smoother operator H^γ .

Lemma 3. $\forall \xi > 0$, the solution $\widehat{H}_\xi^{\gamma, m}$ to $\widehat{\mathcal{E}}_\xi^{\gamma, m}$ exist, and is unique for each γ . Let $\widehat{\mathbf{T}} = \frac{1}{m} \sum_{l=1}^m T_{\widehat{\psi}_{\gamma, l}}$, $\widehat{\mathbf{g}} = \frac{1}{m} \sum_{l=1}^m \Omega_{\widehat{\psi}_{\gamma, l}} \widehat{y}_{\gamma, l}$. Equation (21) has the form

$$\widehat{H}_\xi^{\gamma, m} = (\widehat{\mathbf{T}} + \xi)^{-1} \circ \widehat{\mathbf{g}}.$$

Condition 4. For c_1, c_2 set in Conditions 1– 2 and ι satisfying Condition 3, assume $n_2 \geq \frac{\iota(c_1-1)(c_2+1)}{(c_1+1)(c_2-1)} n_1$.

Remark 1. Condition 4 is sufficient but not necessary to ensure that the error propagates to regression stage from estimating E_Y^p is smaller than that from estimating E_X^p in disjoint sample sets projection.

The main challenge of extending the convergence rate of KIV estimator [Singh et al., 2019] to KAR estimator is that in our case, the excess error depends not only on the accuracy of E_X^p estimator but also on the accuracy of E_Y^p estimator. However, by assuming Condition 4, we ensure the error from estimating E_Y^p is dominated by that of E_X^p , and manage to illustrate the optimal convergence rate for KAR as shown below in Theorem 1.

Theorem 1. Under Condition 1– 4, let $d_1, d_2 > 0$ and choose $\alpha_1 = n_1^{-\frac{1}{c_1+1}}$, $\alpha_2 = n_2^{-\frac{1}{c_2+1}}$, $n_1 = m^{\frac{d_1(c_1+1)}{\iota(c_1-1)}}$, $n_2 = m^{\frac{d_2(c_2+1)}{\iota(c_2-1)}}$, We have:

- (i) If $d_1 \leq \frac{b_\gamma(c_\gamma+1)}{b_\gamma c_\gamma+1}$, then $\mathcal{E}^\gamma(\widehat{H}_\xi^{\gamma,m}) - \mathcal{E}^\gamma(H^\gamma) = O_p(m^{-\frac{d_1 c_\gamma}{c_\gamma+1}})$ with $\xi = m^{-\frac{d_1}{c_\gamma+1}}$.
- (ii) If $d_1 > \frac{b_\gamma(c_\gamma+1)}{b_\gamma c_\gamma+1}$, then $\mathcal{E}^\gamma(\widehat{H}_\xi^{\gamma,m}) - \mathcal{E}^\gamma(H^\gamma) = O_p(m^{-\frac{b_\gamma c_\gamma}{b_\gamma c_\gamma+1}})$ with $\xi = m^{-\frac{b_\gamma}{b_\gamma c_\gamma+1}}$.

At $d_1 = b_\gamma(c_\gamma+1)/(b_\gamma c_\gamma+1) < 2$, the convergence rate of KAR estimator $m^{-b_\gamma c_\gamma/(b_\gamma c_\gamma+1)}$ is optimal. This statistically efficient rate is calibrated by b_γ , the effective input dimension, together with c_γ , the smoothness of the operator H^γ . The condition $d_1 = b_\gamma(c_\gamma+1)/(b_\gamma c_\gamma+1) < 2$ also suggests that $n_1 > m$.

Additional results and discussions including the two-stage approach are included in the Appendix.

4.2 Causal effect and target KAR estimate

In this section, we discuss the scenarios assuming that the data are generated from a structural causal model with nonlinear features as shown below,

$$\begin{pmatrix} C \\ \psi(X) \\ Y \end{pmatrix} = B \begin{pmatrix} \phi(Z) \\ C \\ \psi(X) \\ Y \end{pmatrix} + \begin{pmatrix} \epsilon_C \\ \epsilon_X \\ \epsilon_Y \end{pmatrix}, \quad (22)$$

where we write operator B in the following matrix form

$$B = \begin{pmatrix} B_{CZ} & 0 & 0 & 0 \\ B_{XZ} & B_{XC} & 0 & 0 \\ B_{YZ} & B_{YC} & B_{YX} & 0 \end{pmatrix}.$$

We note that each operator $B_{\Delta\square}$ represents an operator that takes an element from \square -related space to Δ -related space, e.g. $B_{XZ} : \mathcal{H}_Z \rightarrow \mathcal{H}_X$ and $B_{YZ} : \mathcal{H}_Z \rightarrow \mathcal{Y}$. The noise variables ϵ_Z , ϵ_C , ϵ_X and ϵ_Y are independent of each other. Let Σ_Z , Σ_C , Σ_X and Σ_Y denote the covariance of ϵ_Z , ϵ_C , ϵ_X and ϵ_Y , respectively. Here each operator in B represents a line in the model shown in Figure 2. For instance, B_{CZ} stands for the line from \mathcal{H}_Z to C ; B_{YX} corresponds to the line from \mathcal{H}_X to Y . B_{YX} in Equation (22) reflects the causal effect we are interested in. We study the identifiability scenarios where operator B_{YX} can be learned via KAR estimator H^γ .

Theorem 2. An operator B_{XZ} is a zero operator written by $B_{XZ} = 0$, if $\langle \psi(x), B_{XZ}\phi(z) \rangle_{\mathcal{H}_X} = 0$, $\forall \psi(X) \in \mathcal{H}_X, \phi(z) \in \mathcal{H}_Z$. Operator $B_{CZ} = 0$ if $c^\top B_{CZ}\phi(z) = 0$, $\forall c \in \mathcal{C}, \phi(z) \in \mathcal{H}_Z$. A matrix-valued operator, e.g. $B_{YC} = 0$ if all entries are 0. For data generation process following Equation (22), we have $H^\gamma = B_{YX}$ in following cases.

- (i) $B_{YC} = 0$ and $\gamma = 0$, i.e. no latent confounder.
- (ii) $B_{YZ} + B_{YC}B_{CZ} = 0$ and $\gamma = \infty$, where kernel IV is a special case, i.e. both $B_{YZ} = 0$ and $B_{CZ} = 0$.
- (iii) $B_{YC} = 0$, $B_{YZ} + B_{YC}B_{CZ} = 0$, and $\gamma \geq 0$.
- (iv) $\Sigma_{YX}^\parallel = -a\Sigma_{YX}^\perp$ for some $a > 0$, and $\gamma = 1/a$.
 $\Sigma_{YX}^\parallel = (B_{YZ} + B_{YC}B_{CZ})\Sigma_Z(B_{ZX} + B_{ZC}B_{CX})$ denotes the covariance between $\psi(X)$ and Y projected on the linear span from the components of $\phi(Z)$; and $\Sigma_{YX}^\perp = B_{YC}\Sigma_C B_{CX}$ denote the covariance between the residuals of $\psi(X)$ and Y .

Theorem 2 (i) suggests that KPA is optimal when there is no unobserved confounder; (ii) is a generalized condition including KIV; (iii) shows the KAR estimator identifies the causal relation from X to Y regardless of γ with generalized KIV condition in (ii) and no latent confounder in (i); (iv) shows the KAR identifiability condition with appropriate choice of γ when Σ_{XY}^\parallel and Σ_{XY}^\perp are in the flipped direction. In the next section, we show the empirical results for KAR and relevant baseline methods.

5 Empirical Results

5.1 Synthetic experiments

We consider the data generating process of the following nonlinear structural equation,

$$Y = 0.75C - 0.25Z + \ln(|16X - 8| + 1) \text{sgn}(X - 0.5),$$

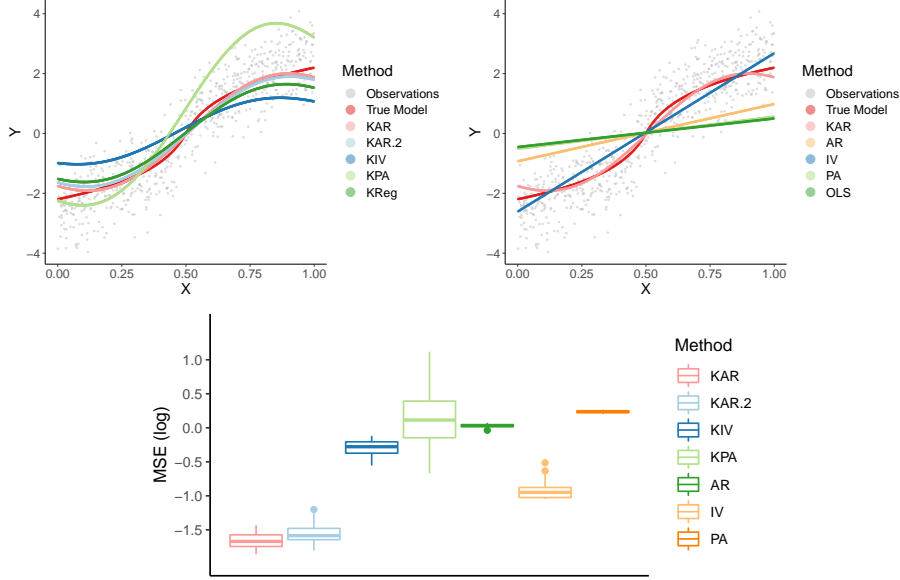


Figure 3: Restuls for the synthetic example: fitted (top left) nonlinear models; and (top right) linear models; (bottom): log MSE.

where $sgn(x) \in \{-1, 0, +1\}$ denotes the sign of x . The explanatory variables X, Z, C are generated from

$$\begin{pmatrix} C \\ V \\ W \end{pmatrix} \sim N \left(\begin{pmatrix} 0 \\ 0 \\ 0 \end{pmatrix}, \begin{pmatrix} 1, 0.3, 0.2 \\ 0.3, 1, 0 \\ 0.2, 0, 1 \end{pmatrix} \right),$$

$$X = F \left(\frac{W + V}{\sqrt{2}} \right), \quad Z = F(W) - 0.5,$$

where F denote the c.d.f of standard normal distribution.

We generate $\{(x_i, y_i, z_i)\}_{i \in [N]}$ samples with $N = 700$. To perform the data-splitting procedures described in Section 3, we set $n_1 = n_2 = 250$ and $n = 500$ for a fair comparison in the projection stage (Section 3.1); and $m = 200$ in the regression stage (Section 3.2). We set regularizers as $\alpha_1 = 1.5n_1^{-0.5}$, $\alpha_2 = 1.5n_2^{-0.5}$, $\alpha = 1.5n^{-0.5}$ and $\xi = 1.5m^{-0.5}$.

Fitting methods We consider estimations via the three-stage kernel anchor regression with disjoint data set projection (**KAR**) and two-stage kernel anchor regression with joint data set projection (**KAR.2**). The baseline approaches include the kernel-based nonlinear methods: kernel instrument variable regression (**KIV**), kernel partialling out regression (**KPA**), kernel ridge regression (**KReg**); and the linear models: linear anchor regression (**AR**), linear instrument variable regression (**IV**), linear partialling out regression (**PA**) and ordinary least square (**OLS**). We use Gaussian kernel for all kernel methods, where the median heuristic is used for choosing

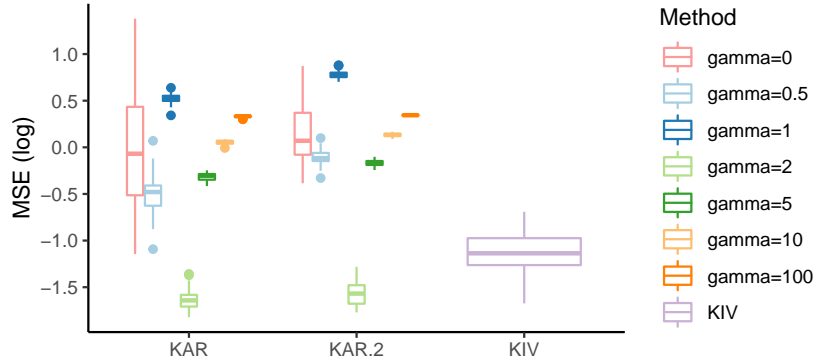


Figure 4: Effects of different γ choices on MSE.

the bandwidth [Gretton et al., 2012]. For the synthetic example, we set $\gamma = 2$ for all anchor regressions (**KAR**, **KAR.2** and **AR**).

For each algorithm, we implement 50 trials and calculate the mean squared error (MSE) with respect to the true causal model $\mathbb{E}(Y|do(x))^4$, which can be computed from the structural model. A trial is shown in Figure 3 as a visual example. We can see that the **KAR** produces a closest estimation to the true model among all other methods and outperforms **KAR.2**. The comparison with linear models are also shown. IV model fits better than other linear models. We report $\log_{10}(\text{MSE})$ in the bottom of Figure 3, which shows that both **KAR** methods have smaller errors than others. **KAR** performs slightly better than **KAR.2** in this case. To check the robustness of **KAR** estimators, we study a less smooth variant of the generating process and show the results in Appendix B.2.

The effect of γ choices To investigate how the change of γ affects the estimator, we consider **KIV** as our baseline as the IV setting corresponds to $\gamma \rightarrow \infty$. We consider the data generating process used in the **KIV** paper [Singh et al., 2019]. The $\log_{10}(\text{MSE})$ results of **KAR** and **KAR.2**, in comparison with **KIV**, are shown in Figure 4. For the simulation, we set $N = 1000$, $n_1 = n_2 = 200$, $n = n_1 + n_2 = 400$ and $m = 600$. From the result, we can see that both **KAR** and **KAR.2** achieves smaller error when choosing $\gamma = 2$. Data generation and model implementation details are included in Appendix B.1.

Intervention and Generalization To evaluate the robustness and generalization performance of both **KAR** estimators under distribution shift, as discussed in Rothenhäusler et al. [2018], we intervene the anchor variable Z . We train the model on a subpopulation of samples with $Z < 0$

⁴Setting a particular value $X = x$ while ignoring other variables that may potentially changing the distribution of y , $p(y|X = x)$ is noted as $p(y|do(x))$ [Pearl, 2009; Peters et al., 2016]. $\mathbb{E}[Y|do(x)]$ is set as the mean over $p(y|do(x))$ averaging out different Z values in this case.

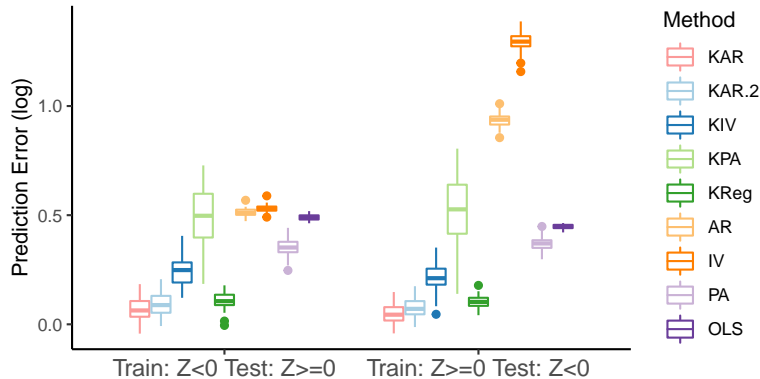


Figure 5: Prediction error with distributional intervention.

and test on the samples with $Z \geq 0$. The performance is measured by prediction error (PE) of fitted model with respect to $\mathbb{E}(Y|X = x, Z \geq 0)$, where the true conditional model is not known in closed form but estimated from samples.

We also exchange the training set and the testing set. As shown in Figure 5, our **KAR** estimator has the lowest PE among others, showing better out-of-distribution generalization performance. More importantly, by checking the two (flipped) scenarios, i.e. train on $Z < 0$ v.s. train on $Z \geq 0$, we also see that **KAR** is the most invariant in terms of PE. On the contrary, linear version of **AR** and **IV** achieves very different PE in both cases. Variances of PE for **KPA** are also very different in the two cases. Despite **KReg** achieves a relatively low PE in both cases, the distributions of PE can be found very different.

5.2 Real-world application

We consider the smoking dataset extracted from National Medical Expenditure Survey (NMES) [Johnson et al., 2003] to study the effect of smoking amount on medical expenditure [Imai and Van Dyk, 2004]⁵.

The treatment variable X is the log of smoking amount, the outcome Y is the log of medical expenditure, and the anchor Z is set to be the last age for smoking. We use 1000 samples, randomly selected from 9708 available samples, to fit the model. We set $n_1 = n_2 = 300$, $n = 600$ and $m = 400$. We also set $\gamma = 2.9$ and apply Gaussian kernel with median heuristic bandwidth [Gretton et al., 2012] for all kernel methods. As shown in the upper part of Figure 6, **KAR** estimators show that the effect of X on Y is more significant when $X \in [-2, 1]$ compared to $X \in [1, 4]$. Our method can also be used in complement with the approaches finding causal

⁵The dataset is accessible through using the R package for “estimating causal dose response function” `causaldrf` [Galagate, 2016] <https://cran.r-project.org/web/packages/causaldrf/index.html>.

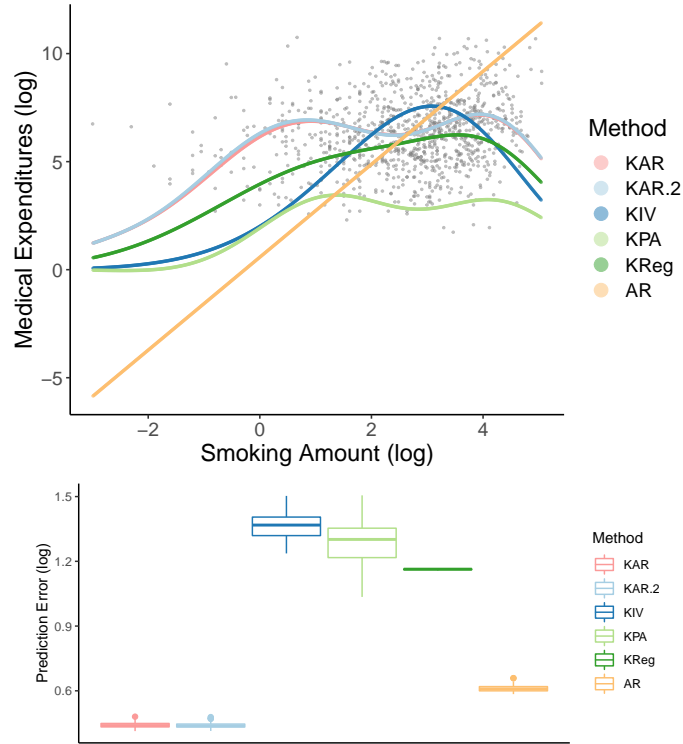


Figure 6: Fitted models (top) and prediction errors (bottom) when training on male subjects and testing on female subjects.

directions, e.g. [Peters et al., 2016]⁶. We run the CAM to ensure that there is a causal effect in the direction from X to Y and KAR procedure further learns the specific function representing such effect. However, existing work such as propensity score approaches [Imai and Van Dyk, 2004] did not manage to extract such causal relationship between smoking and medical expenditure.

To strengthen our finding, we quantify the performance of the estimators. Since we do not know the real generating process of the data, we cannot compare the MSE as Figure 3 and 4. Instead, it's feasible to evaluate the performance of estimators under distribution perturbation via PE, similar to Figure 5. We train models on male subjects and compute the prediction accuracy of fitted model on female subjects. The results are shown in the bottom of Figure 6. From the result, we see that both KAR approaches outperform other kernel-based approaches as well as the linear version of AR, suggesting a better learned effect from the smoking amount to medical expenditure.

⁶Implementation with R package CAM can be found at <https://rdr.io/cran/CAM/man/CAM.html>

6 Conclusion

In this work, we consider learning a more general class of causal DAG in a nonlinear setting using kernelized anchor regression. By considering different data splitting strategies to estimate the projection operators, we show that the three-stage approach not only performs better empirically than baseline approaches as well as the 2SLS approach, but also achieves optimal rate under given conditions. Identifiability results are provided and are shown to generalize KIV and “no latent confounder” scenarios. For the future, data adaptive choice of γ can be an interesting direction to explore.

Acknowledgements

The authors thank Ana Korba for helpful discussions. W.X. acknowledges the support from EPSRC grant EP/T018445/1.

References

- Angrist, J. D., Imbens, G. W., and Rubin, D. B. (1996). Identification of causal effects using instrumental variables. *Journal of the American statistical Association*, 91(434):444–455.
- Arjovsky, M., Bottou, L., Gulrajani, I., and Lopez-Paz, D. (2019). Invariant risk minimization. *arXiv preprint arXiv:1907.02893*.
- Bennett, A., Kallus, N., and Schnabel, T. (2019). Deep generalized method of moments for instrumental variable analysis. *Advances in neural information processing systems*, 32.
- Beserve, M., Mehrjou, A., Sun, R., and Schölkopf, B. (2019). Counterfactuals uncover the modular structure of deep generative models. In *International Conference on Learning Representations*.
- Bishop, C. M. (1998). Latent variable models. In *Learning in graphical models*, pages 371–403. Springer.
- Blei, D. M. (2012). Probabilistic topic models. *Communications of the ACM*, 55(4):77–84.
- Bowden, R. J. and Turkington, D. A. (1990). *Instrumental variables*. Number 8. Cambridge university press.
- Bühlmann, P. (2018). Invariance, causality and robustness. *arXiv preprint arXiv:1812.08233*.
- Centorrino, S., Fève, F., and Florens, J.-P. (2019). Nonparametric instrumental regressions with (potentially discrete) instruments independent of the error term. *arXiv preprint arXiv:1905.07812*.

- Chen, X. and Christensen, T. M. (2018). Optimal sup-norm rates and uniform inference on nonlinear functionals of nonparametric iv regression. *Quantitative Economics*, 9(1):39–84.
- Chernozhukov, V., Fernández-Val, I., and Melly, B. (2013). Inference on counterfactual distributions. *Econometrica*, 81(6):2205–2268.
- Colombo, D., Maathuis, M. H., Kalisch, M., and Richardson, T. S. (2012). Learning high-dimensional directed acyclic graphs with latent and selection variables. *The Annals of Statistics*, pages 294–321.
- Fukumizu, K., Gretton, A., Sun, X., and Schölkopf, B. (2007). Kernel measures of conditional dependence. *Advances in neural information processing systems*, 20.
- Galagate, D. (2016). *Causal inference with a continuous treatment and outcome: Alternative estimators for parametric dose-response functions with applications*. PhD thesis, University of Maryland, College Park.
- Glymour, C., Zhang, K., and Spirtes, P. (2019). Review of causal discovery methods based on graphical models. *Frontiers in genetics*, 10:524.
- Gretton, A., Borgwardt, K. M., Rasch, M. J., Schölkopf, B., and Smola, A. (2012). A kernel two-sample test. *The Journal of Machine Learning Research*, 13(1):723–773.
- Gretton, A., Bousquet, O., Smola, A., and Schölkopf, B. (2005). Measuring statistical dependence with hilbert-schmidt norms. In *International conference on algorithmic learning theory*, pages 63–77. Springer.
- Grünewälder, S., Lever, G., Baldassarre, L., Patterson, S., Gretton, A., and Pontil, M. (2012). Conditional mean embeddings as regressors. In *Proceedings of the 29th International Conference on Machine Learning*, pages 1803–1810.
- Hartford, J., Lewis, G., Leyton-Brown, K., and Taddy, M. (2017). Deep IV: A flexible approach for counterfactual prediction. In *International Conference on Machine Learning*, pages 1414–1423. PMLR.
- Hofmann, T., Schölkopf, B., and Smola, A. J. (2008). Kernel methods in machine learning. *The annals of statistics*, 36(3):1171–1220.
- Hoyer, P., Janzing, D., Mooij, J. M., Peters, J., and Schölkopf, B. (2008). Nonlinear causal discovery with additive noise models. *Advances in neural information processing systems*, 21.
- Hyvärinen, A. (2013). Independent component analysis: recent advances. *Philosophical Transactions of the Royal Society A: Mathematical, Physical and Engineering Sciences*, 371(1984):20110534.

- Hyvärinen, A. and Dayan, P. (2005). Estimation of non-normalized statistical models by score matching. *Journal of Machine Learning Research*, 6(4).
- Hyvarinen, A. and Morioka, H. (2017). Nonlinear ica of temporally dependent stationary sources. In *Artificial Intelligence and Statistics*, pages 460–469. PMLR.
- Hyvärinen, A., Zhang, K., Shimizu, S., and Hoyer, P. O. (2010). Estimation of a structural vector autoregression model using non-gaussianity. *Journal of Machine Learning Research*, 11(5).
- Imai, K. and Van Dyk, D. A. (2004). Causal inference with general treatment regimes: Generalizing the propensity score. *Journal of the American Statistical Association*, 99(467):854–866.
- Johansson, F. D., Shalit, U., Kallus, N., and Sontag, D. (2020). Generalization bounds and representation learning for estimation of potential outcomes and causal effects. *arXiv preprint arXiv:2001.07426*.
- Johnson, E., Dominici, F., Griswold, M., and Zeger, S. L. (2003). Disease cases and their medical costs attributable to smoking: an analysis of the national medical expenditure survey. *Journal of Econometrics*, 112(1):135–151.
- Kallus, N. (2020). Deepmatch: Balancing deep covariate representations for causal inference using adversarial training. In *International Conference on Machine Learning*, pages 5067–5077. PMLR.
- Khemakhem, I., Monti, R., Leech, R., and Hyvarinen, A. (2021). Causal autoregressive flows. In *International conference on artificial intelligence and statistics*, pages 3520–3528. PMLR.
- Kook, L., Sick, B., and Bühlmann, P. (2022). Distributional anchor regression. *Statistics and Computing*, 32(3):1–19.
- Louizos, C., Shalit, U., Mooij, J. M., Sontag, D., Zemel, R., and Welling, M. (2017). Causal effect inference with deep latent-variable models. *Advances in neural information processing systems*, 30.
- Micchelli, C. A. and Pontil, M. (2005). On learning vector-valued functions. *Neural computation*, 17(1):177–204.
- Monti, R. P., Zhang, K., and Hyvärinen, A. (2020). Causal discovery with general non-linear relationships using non-linear ica. In *Uncertainty in artificial intelligence*, pages 186–195. PMLR.
- Mooij, J., Janzing, D., Peters, J., and Schölkopf, B. (2009). Regression by dependence minimization and its application to causal inference in additive noise models. In *Proceedings of the 26th annual international conference on machine learning*, pages 745–752.

- Muandet, K., Fukumizu, K., Sriperumbudur, B., Schölkopf, B., et al. (2017). Kernel mean embedding of distributions: A review and beyond. *Foundations and Trends® in Machine Learning*, 10(1-2):1–141.
- Muandet, K., Kanagawa, M., Saengkyongam, S., and Marukatat, S. (2021). Counterfactual mean embeddings. *Journal of Machine Learning Research*, 22(162):1–71.
- Oberst, M., Thams, N., Peters, J., and Sontag, D. (2021). Regularizing towards causal invariance: Linear models with proxies. In *International Conference on Machine Learning*, pages 8260–8270. PMLR.
- Pearl, J. (2009). *Causality*. Cambridge university press.
- Pearl, J. et al. (2000). Models, reasoning and inference. *Cambridge, UK: CambridgeUniversity-Press*, 19(2).
- Pearl, J., Glymour, M., and Jewell, N. P. (2016). *Causal Inference in Statistics: A Primer*. John Wiley & Sons.
- Peters, J., Bühlmann, P., and Meinshausen, N. (2016). Causal inference by using invariant prediction: identification and confidence intervals. *Journal of the Royal Statistical Society: Series B (Statistical Methodology)*, 78(5):947–1012.
- Peters, J., Janzing, D., and Schölkopf, B. (2017). *Elements of causal inference: foundations and learning algorithms*. MIT press.
- Peters, J., Mooij, J. M., Janzing, D., and Schölkopf, B. (2011). Identifiability of causal graphs using functional models. In *Proceedings of the Twenty-Seventh Conference on Uncertainty in Artificial Intelligence*, pages 589–598.
- Peters, J., Mooij, J. M., Janzing, D., and Schölkopf, B. (2014). Causal discovery with continuous additive noise models. *Journal of Machine Learning Research*, 15:2009–2053.
- Rabiner, L. and Juang, B. (1986). An introduction to hidden markov models. *ieee assp magazine*, 3(1):4–16.
- Rolland, P., Cevher, V., Kleindessner, M., Russell, C., Janzing, D., Schölkopf, B., and Locatello, F. (2022). Score matching enables causal discovery of nonlinear additive noise models. In *International Conference on Machine Learning*, pages 18741–18753. PMLR.
- Rothenhäusler, D., Meinshausen, N., Bühlmann, P., and Peters, J. (2018). Anchor regression: heterogeneous data meets causality. *arXiv preprint arXiv:1801.06229*.
- Rubin, D. B. (2004). Direct and indirect causal effects via potential outcomes. *Scandinavian Journal of Statistics*, 31(2):161–170.

- Rubin, D. B. (2005). Causal inference using potential outcomes: Design, modeling, decisions. *Journal of the American Statistical Association*, 100(469):322–331.
- Schölkopf, B., Locatello, F., Bauer, S., Ke, N. R., Kalchbrenner, N., Goyal, A., and Bengio, Y. (2021). Toward causal representation learning. *Proceedings of the IEEE*, 109(5):612–634.
- Scholkopf, B. and Smola, A. J. (2018). *Learning with kernels: support vector machines, regularization, optimization, and beyond*. MIT press.
- Shimizu, S., Hoyer, P. O., Hyvärinen, A., Kerminen, A., and Jordan, M. (2006). A linear non-gaussian acyclic model for causal discovery. *Journal of Machine Learning Research*, 7(10).
- Shimizu, S., Inazumi, T., Sogawa, Y., Hyvärinen, A., Kawahara, Y., Washio, T., Hoyer, P. O., and Bollen, K. (2011). Directlingam: A direct method for learning a linear non-gaussian structural equation model. *The Journal of Machine Learning Research*, 12:1225–1248.
- Singh, R., Sahani, M., and Gretton, A. (2019). Kernel instrumental variable regression. *arXiv preprint arXiv:1906.00232*.
- Song, L., Huang, J., Smola, A., and Fukumizu, K. (2009). Hilbert space embeddings of conditional distributions with applications to dynamical systems. In *Proceedings of the 26th Annual International Conference on Machine Learning*, pages 961–968.
- Spirtes, P., Glymour, C. N., Scheines, R., and Heckerman, D. (2000). *Causation, prediction, and search*. MIT press.
- Spirtes, P. L., Meek, C., and Richardson, T. S. (2013). Causal inference in the presence of latent variables and selection bias. *arXiv preprint arXiv:1302.4983*.
- Steinwart, I. and Christmann, A. (2008). *Support vector machines*. Springer Science & Business Media.
- Szabó, Z., Gretton, A., Póczos, B., and Sriperumbudur, B. (2015). Two-stage sampled learning theory on distributions. In *Artificial Intelligence and Statistics*, pages 948–957. PMLR.
- Szabó, Z., Sriperumbudur, B. K., Póczos, B., and Gretton, A. (2016). Learning theory for distribution regression. *The Journal of Machine Learning Research*, 17(1):5272–5311.
- Xu, L., Chen, Y., Srinivasan, S., de Freitas, N., Doucet, A., and Gretton, A. (2020). Learning deep features in instrumental variable regression. *arXiv preprint arXiv:2010.07154*.
- Xu, L., Kanagawa, H., and Gretton, A. (2021). Deep proxy causal learning and its application to confounded bandit policy evaluation. *Advances in Neural Information Processing Systems*, 34:26264–26275.

Zhang, K., Schölkopf, B., Spirtes, P., and Glymour, C. (2018). Learning causality and causality-related learning: some recent progress. *National science review*, 5(1):26–29.

Zhu, Y., Gultchin, L., Gretton, A., Kusner, M. J., and Silva, R. (2022). Causal inference with treatment measurement error: a nonparametric instrumental variable approach. In *Uncertainty in Artificial Intelligence*, pages 2414–2424. PMLR.

Supplementary Material for Nonlinear Causal Discovery via Kernel Anchor Regression

A Proofs and derivations

A.1 Proof of Theorem 1

Before proving Theorem 1, we introduce the exact bounds of the approximation errors for estimating E_X^p and E_Y^p in the disjoint sample sets projection stage. Lemma A1 and A2 below are adapted from Theorem 2 in Singh et al. [2019].

Lemma A1. Under Condition 1, $\forall \delta \in (0, 1)$, the following holds w.p. $1 - \delta$:

$$\|E_{\alpha_1, X}^{n_1} - E_X^p\|_{\mathcal{H}_\Gamma} \leq r_{E_1}(\delta, n_1, c_1) := \frac{\sqrt{\zeta_1}(c_1 + 1)}{4^{\frac{1}{c_1+1}}} \left(\frac{4\kappa(Q_1 + \kappa\|E_X^p\|_{\mathcal{H}_\Gamma} \ln(2/\delta))}{\sqrt{n_1\zeta_1}(c_1 - 1)} \right)^{\frac{c_1-1}{c_1+1}},$$

$$\alpha_1 = \left(\frac{8\kappa(Q_1 + \kappa\|E_X^p\|_{\mathcal{H}_\Gamma} \ln(2/\delta))}{\sqrt{n_1\zeta_1}(c_1 - 1)} \right)^{\frac{2}{c_1+1}}.$$

Lemma A2. Under Condition 1 and Condition 2, $\forall \epsilon \in (0, 1)$, the following holds w.p. $1 - \epsilon$:

$$\|E_{\alpha_2, Y}^{n_2} - E_Y^p\|_{\mathcal{H}_\Theta} \leq r_{E_2}(\epsilon, n_2, c_2) := \frac{\sqrt{\zeta_2}(c_2 + 1)}{4^{\frac{1}{c_2+1}}} \left(\frac{4\kappa(Q_2 + \kappa\|E_Y^p\|_{\mathcal{H}_\Theta} \ln(2/\epsilon))}{\sqrt{n_2\zeta_2}(c_2 - 1)} \right)^{\frac{c_2-1}{c_2+1}},$$

$$\alpha_2 = \left(\frac{8\kappa(Q_2 + \kappa\|E_Y^p\|_{\mathcal{H}_\Theta} \ln(2/\epsilon))}{\sqrt{n_2\zeta_2}(c_2 - 1)} \right)^{\frac{2}{c_2+1}}.$$

Recall that we define the population-level risk for the regression stage $\mathcal{E}^\gamma(H)$, population-level risk with regularization $\mathcal{E}_\xi^\gamma(H)$, and the empirical risk $\widehat{\mathcal{E}}_\xi^{\gamma, m}(H)$ with E_X^p and E_Y^p being replaced by $E_{\alpha_1, X}^{n_1}$ and $E_{\alpha_2, Y}^{n_2}$, respectively. Denote the optimal operator to $\mathcal{E}_\xi^\gamma(H)$ as $H_\xi^\gamma = \arg \min_H \mathcal{E}_\xi^\gamma(H)$. We now define the empirical risk $\mathcal{E}_{\gamma, m}^\xi(H)$ with true E_X^p and E_Y^p , and the corresponding optimal operator.

$$\mathcal{E}_\xi^{\gamma, m}(H) = \frac{1}{m} \sum_{l=1}^m \|y_{\gamma, l} - H\psi_{\gamma, l}\|_{\mathcal{Y}}^2 + \xi \|H\|_{\mathcal{H}_\Omega}^2, \quad H_\xi^{\gamma, m} = \arg \min_H \mathcal{E}_\xi^{\gamma, m}(H),$$

where the true transformed inputs and outputs are given by

$$\psi_{\gamma, l} = \psi(x_l) + (\sqrt{\gamma} - 1)E_X^p\phi(z_l) \in \mathcal{H}_X, \quad y_{\gamma, l} = y_l + (\sqrt{\gamma} - 1)E_Y^p\phi(z_l) \in \mathcal{Y}.$$

The closed form solution of $H_\xi^{\gamma, m}$ is given by Lemma A3 below, and it's adapted from Theorem 3 in Singh et al. [2019]

Lemma A3. $\forall \xi > 0$, the solution $H_\xi^{\gamma, m}$ to $\mathcal{E}_\xi^{\gamma, m}$ exists, is unique, and

$$\mathbf{T} = \frac{1}{m} \sum_{l=1}^m T_{\psi_{\gamma, l}}, \quad \mathbf{g} = \frac{1}{m} \sum_{l=1}^m \Omega_{\psi_{\gamma, l}} y_{\gamma, l}, \quad H_\xi^{\gamma, m} = (\mathbf{T} + \xi)^{-1} \circ \mathbf{g}.$$

We then define the following terms.

Definition 1. Fix $\eta \in (0, 1)$ and define the following constants

$$C_\eta = 96 \ln^2(6/\eta), \quad M = 2(C + \|H^\gamma\|_{\mathcal{H}_\Omega} \sqrt{B}), \quad \Sigma = \frac{M}{2}.$$

For the excess error of **KAR** estimator $\widehat{H}_\xi^{\gamma, m}$, we can bound it by five terms according to Proposition 32 in [Singh et al. \[2019\]](#).

Lemma A4. The excess error can be bounded as follows

$$\mathcal{E}^\gamma(\widehat{H}_\xi^{\gamma, m}) - \mathcal{E}^\gamma(H^\gamma) \leq 5[S_{-1} + S_0 + \mathcal{A}(\xi) + S_1 + S_2],$$

where

$$\begin{aligned} S_{-1} &= \|\sqrt{T} \circ (\widehat{\mathbf{T}} + \xi)^{-1} (\widehat{\mathbf{g}} - \mathbf{g})\|_{\mathcal{H}_\Omega}^2, \\ S_0 &= \|\sqrt{T} \circ (\widehat{\mathbf{T}} + \xi)^{-1} (\mathbf{T} - \widehat{\mathbf{T}}) H_\xi^{\gamma, m}\|_{\mathcal{H}_\Omega}^2, \\ S_1 &= \|\sqrt{T} \circ (\widehat{\mathbf{T}} + \xi)^{-1} (\mathbf{g} - \mathbf{T} H^\gamma)\|_{\mathcal{H}_\Omega}^2, \\ S_2 &= \|\sqrt{T} \circ (\widehat{\mathbf{T}} + \xi)^{-1} (T - \mathbf{T})(H_\xi^\gamma - H^\gamma)\|_{\mathcal{H}_\Omega}^2, \\ \mathcal{A}(\xi) &= \|\sqrt{T}(H_\xi^\gamma - H^\gamma)\|_{\mathcal{H}_\Omega}^2. \end{aligned}$$

For all five terms above, only $\widehat{\mathbf{g}} - \mathbf{g}$ in S_{-1} depends on the approximation error of E_Y^p . The bounds for other four terms are same to the **KIV** case. Below we introduce without proof the bound of S_0, S_1, S_2 and $\mathcal{A}(\xi)$ according to Theorem 7 in [Singh et al. \[2019\]](#).

Lemma A5. Under Condition 1–3, if m is large enough and $\xi \leq \|T\|_{L(\mathcal{H}_\Omega)}$ then $\forall \delta, \eta \in (0, 1)$, the following holds up w.p. $1 - \eta - \delta$:

$$\begin{aligned} S_0 &\leq \frac{4}{\xi} 4BL^2 r_x^{2\iota} \|H_\xi^{\gamma, m}\|_{\mathcal{H}_\Omega}^2, \\ S_1 &\leq 32 \ln^2(6\eta) \left[\frac{BM^2}{m^2 \xi} + \frac{\Sigma^2}{m} \beta^{1/b_\gamma} \frac{\pi/b_\gamma}{\sin(\pi) \xi^{-1/b_\gamma}} \right], \\ S_2 &\leq 8 \ln^2(6\eta) \left[\frac{4B^2 \zeta \xi^{c_\gamma - 1}}{m^2 \xi} + \frac{B \zeta \xi^{c_\gamma}}{m \xi} \right], \\ \mathcal{A}(\xi) &\leq \zeta \xi^{c_\gamma}. \end{aligned}$$

To extend the convergence rate of **KIV** estimator to **KAR** estimator. We then illustrate the bound for S_{-1} . To begin with, the bound of term $\sqrt{T} \circ (\widehat{\mathbf{T}} + \xi)^{-1}$ in S_{-1} is given by Proposition 39 in [Singh et al. \[2019\]](#).

Lemma A6. If $\|\widehat{\psi}_\gamma - \psi_\gamma\|_{\mathcal{H}_X} \leq r_x$ w.p. $1 - \delta$, $\xi \leq \|T\|_{L(\mathcal{H}_\Omega)}$, m is sufficiently large and Condition 3 holds, then w.p. $1 - \eta/3 - \delta$

$$\|\sqrt{T} \circ (\widehat{\mathbf{T}} + \xi)^{-1}\|_{L(\mathcal{H}_\Omega)} \leq \frac{2}{\sqrt{\xi}}.$$

With the the error propagated from the estimators in the projection stage, we can bound $\widehat{\psi}_\gamma - \psi_\gamma$ and $\widehat{y}_\gamma - y_\gamma$ as shown in Lemma A7–A8.

Lemma A7. Under Condition 1, $\forall \delta \in (0, 1)$, the following statement holds w.p. $1 - \delta$: $\forall z \in \mathcal{Z}, x \in \mathcal{X}$,

$$\|\widehat{\psi}_\gamma - \psi_\gamma\|_{\mathcal{H}_X} \leq r_x(\gamma, \delta, n_1, c_1) := |\sqrt{\gamma} - 1| \kappa r_{E_1}(\delta, n_1, c_1).$$

Proof. By definition, we have

$$\begin{aligned} \|\widehat{\psi}_\gamma - \psi_\gamma\|_{\mathcal{H}_X} &= \|(\sqrt{\gamma} - 1) (E_{\alpha_1, X}^{n_1} - E_X^p) \phi(z)\|_{\mathcal{H}_X} \\ &\leq |\sqrt{\gamma} - 1| \|E_{\alpha_1, X}^{n_1} - E_X^p\|_{\mathcal{H}_\Gamma} \|\phi(z)\|_{\mathcal{H}_Z}. \end{aligned}$$

This, together with Lemma A1 and Condition 1, ensures that w.p. $1 - \delta$

$$\|\widehat{\psi}_\gamma - \psi_\gamma\|_{\mathcal{H}_X} \leq r_x(\gamma, \delta, n_1, c_1) := |\sqrt{\gamma} - 1| \kappa r_{E_1}(\delta, n_1, c_1).$$

□

Remark A1. Corollary 1 in Singh et al. [2019] is a special case of Lemma A7 with $\gamma = 0$.

Lemma A8. Under Condition 1–2, $\forall \epsilon \in (0, 1)$, the following statement holds w.p. $1 - \epsilon$: $\forall z \in \mathcal{Z}, y \in \mathcal{Y}$,

$$\|\widehat{y}_\gamma - y_\gamma\|_{\mathcal{H}_Y} \leq r_y(\gamma, \epsilon, n_2, c_2) := |\sqrt{\gamma} - 1| \kappa r_{E_2}(\epsilon, n_2, c_2).$$

Proof. Lemma A8 is analogous to Lemma A7 by replacing ψ_γ with y_γ . The proof is thus omitted. □

Combining Lemma A6–A8, we can derive the bound of $\widehat{\mathbf{g}} - \mathbf{g}$ and then the bound of S_{-1} .

Lemma A9. If $\|\widehat{\psi}_\gamma - \psi_\gamma\|_{\mathcal{H}_X} \leq r_x$ w.p. $1 - \delta$ and $\|\widehat{y}_\gamma - y_\gamma\|_{\mathcal{Y}} \leq r_y$ w.p. $1 - \epsilon$, then w.p. $1 - \delta - \epsilon$

$$\|\widehat{\mathbf{g}} - \mathbf{g}\|_{\mathcal{H}_\Omega}^2 \leq 3(L^2 r_x^{2\iota} r_y^2 + B^2 r_y^2 + L^2 r_x^{2\iota} C^2).$$

Proof. By definition, we have

$$\begin{aligned} \widehat{\mathbf{g}} - \mathbf{g} &= \frac{1}{m} \sum_{l=1}^m \left(\Omega_{\widehat{\psi}_{\gamma, l}} \widehat{y}_{\gamma, l} - \Omega_{\psi_{\gamma, l}(x)} y_{\gamma, l} \right) \\ &= \frac{1}{m} \sum_{l=1}^m \left\{ \Omega_{\widehat{\psi}_{\gamma, l}} - \Omega_{\psi_{\gamma, l}} \right\} \{ \widehat{y}_{\gamma, l} - y_{\gamma, l} \} + \Omega_{\widehat{\psi}_{\gamma, l}} \{ \widehat{y}_{\gamma, l} - y_{\gamma, l} \} + \left\{ \Omega_{\widehat{\psi}_{\gamma, l}} - \Omega_{\psi_{\gamma, l}} \right\} y_{\gamma, l}. \end{aligned}$$

We then have

$$\begin{aligned}
\|\widehat{\mathbf{g}} - \mathbf{g}\|_{\mathcal{H}_\Omega}^2 &\leq \frac{3m}{m^2} \sum_{l=1}^m \left\| \left\{ \Omega_{\widehat{\psi}_{\gamma,l}} - \Omega_{\psi_{\gamma,l}} \right\} \{\widehat{y}_{\gamma,l} - y_{\gamma,l}\} \right\|_{\mathcal{H}_\Omega}^2 + \|\Omega_{\widehat{\psi}_{\gamma,l}} \{\widehat{y}_{\gamma,l} - y_{\gamma,l}\}\|_{\mathcal{H}_\Omega}^2 \\
&\quad + \left\| \left\{ \Omega_{\widehat{\psi}_{\gamma,l}} - \Omega_{\psi_{\gamma,l}} \right\} y_{\gamma,l} \right\|_{\mathcal{H}_\Omega}^2 \\
&\leq \frac{3}{m} \sum_{l=1}^m \|\Omega_{\widehat{\psi}_{\gamma,l}} - \Omega_{\psi_{\gamma,l}}\|_{L(\mathcal{Y}, \mathcal{H}_\Omega)}^2 \|\widehat{y}_{\gamma,l} - y_{\gamma,l}\|_{\mathcal{Y}}^2 + \|\Omega_{\psi_{\gamma,l}}\|_{L(\mathcal{Y}, \mathcal{H}_\Omega)}^2 \|\widehat{y}_{\gamma,l} - y_{\gamma,l}\|_{\mathcal{Y}}^2 \\
&\quad + \|\Omega_{\widehat{\psi}_{\gamma,l}} - \Omega_{\psi_{\gamma,l}}\|_{L(\mathcal{Y}, \mathcal{H}_\Omega)}^2 \|y_{\gamma,l}\|_{\mathcal{Y}}^2.
\end{aligned}$$

By the boundedness and the Hölder property in Condition 3, we obtain that w.p. $1 - \delta - \epsilon$,

$$\begin{aligned}
\|\widehat{\mathbf{g}} - \mathbf{g}\|_{\mathcal{H}_\Omega}^2 &\leq \frac{3}{m} \sum_{l=1}^m L^2 \|\widehat{\psi}_{\gamma,l} - \psi_{\gamma,l}\|_{\mathcal{H}_X}^{2\iota} \|\widehat{y}_{\gamma,l} - y_{\gamma,l}\|_{\mathcal{Y}}^2 + \|\Omega_{\psi_{\gamma,l}}\|_{L(\mathcal{Y}, \mathcal{H}_\Omega)}^2 \|\widehat{y}_{\gamma,l} - y_{\gamma,l}\|_{\mathcal{Y}}^2 \\
&\quad + L^2 \|\widehat{\psi}_{\gamma,l} - \psi_{\gamma,l}\|_{\mathcal{H}_X}^{2\iota} \|y_{\gamma,l}\|_{\mathcal{Y}}^2 \\
&\leq 3(L^2 r_x^{2\iota} r_y^2 + B^2 r_y^2 + L^2 r_x^{2\iota} C^2).
\end{aligned}$$

□

Lemma A10. Under Condition 1–3, then w.p. $1 - \delta - \epsilon$

$$S_{-1} \leq \frac{4}{\xi} 3(L^2 r_x^{2\iota} r_y^2 + B^2 r_y^2 + L^2 r_x^{2\iota} C^2).$$

Proof. We can derive from the definition of S_{-1} that

$$S_{-1} \leq \|\sqrt{T} \circ (\widehat{\mathbf{T}} + \xi)^{-1}\|_{L(\mathcal{H}_\Omega)}^2 \|\widehat{\mathbf{g}} - \mathbf{g}\|_{\mathcal{H}_\Omega}^2.$$

This, together with Lemma A6 and Lemma A9, ensures

$$S_{-1} \leq \frac{4}{\xi} 3(L^2 r_x^{2\iota} r_y^2 + B^2 r_y^2 + L^2 r_x^{2\iota} C^2).$$

□

We then show the order of the sum $S_0 + S_1 + S_2 + \mathcal{A}(\xi)$, which is adapted from Theorem 4 in Singh et al. [2019].

Lemma A11. Under Condition 1– 3, choose $\alpha_1 = n_1^{-\frac{1}{c_1+1}}$, $n_1 = m^{\frac{d_1(c_1+1)}{\iota(c_1-1)}}$, where $d_1 > 0$. Let

$$f(m) = \frac{1}{m^{2+d_1} \xi^3} + \frac{1}{m^{1+d_1} \xi^{2+1/b_\gamma}} + \frac{1}{m^{d_1} \xi} + \xi^{c_\gamma} + \frac{1}{m^2 \xi} + \frac{1}{m \xi^{1/b_\gamma}},$$

we then have

$$O_p(S_0 + \mathcal{A}(\xi) + S_1 + S_2) = O(f(m)).$$

- (i) If $d_1 \leq \frac{b_\gamma(c_\gamma+1)}{b_\gamma c_\gamma+1}$ then $O(f(m)) = O(m^{-\frac{d_1 c_\gamma}{c_\gamma+1}})$ with $\xi = m^{-\frac{d_1}{c_\gamma+1}}$;
- (ii) If $d_1 > \frac{b_\gamma(c_\gamma+1)}{b_\gamma c_\gamma+1}$ then $O(f(m)) = O(m^{-\frac{b_\gamma c_\gamma}{b_\gamma c_\gamma+1}})$ with $\xi = m^{-\frac{b_\gamma}{b_\gamma c_\gamma+1}}$.

Proof of Theorem 1. The choices of α_1, α_2 and n_1, n_2 in the statement of Theorem 1 ensure that

$$r_x^2 = O([(n_1^{-\frac{1}{2}})^{\frac{2}{c_1+1}}]^{2\iota}) = O(m^{-d_1}), \quad r_y^2 = O([(n_2^{-\frac{1}{2}})^{\frac{2}{c_2+1}}]^{2\iota}) = O(m^{-d_2}).$$

Thus, by Lemma A10, we have

$$O_p(S_{-1}) = O_p(1/\xi(r_x^{2\iota} r_y^2 + r_y^2 + r_x^{2\iota})) = O_p(1/\xi \{m^{-d_1} + m^{-d_2} + m^{-d_1-d_2}\}).$$

Since $d_1, d_2 > 0$, and $d_1 \leq d_2$ by Condition 4, m^{-d_1}/ξ then dominates two other terms in S_{-1} .

Note that $f(m)$ in Lemma A11 also includes m^{-d_1}/ξ . Therefore, given Condition 4, the sum of four terms $S_0 + \mathcal{A}(\xi) + S_1 + S_2$ dominates S_{-1} , which suggests that the approximation error of E_Y^p is dominated by that of E_X^p . We can then derive the result from Lemma A11. \square

A.2 Proof of Theorem 2

Proof of Theorem 2. Under the kernel structural equation model, simple calculation gives

$$C = B_{CZ}\Phi(Z) + \epsilon_C, \quad (23)$$

$$\Psi(X) = (B_{XZ} + B_{XC}B_{CZ})\Phi(Z) + B_{XC}\epsilon_C + \epsilon_X, \quad (24)$$

$$Y = [B_{YZ} + B_{YC}B_{CZ} + B_{YX}(B_{XZ} + B_{XC}B_{CZ})]\Phi(Z) \\ + (B_{YC} + B_{YX}B_{XC})\epsilon_C + B_{YX}\epsilon_X + \epsilon_Y. \quad (25)$$

We denote $B_{\square\Delta}$ as the adjoint operator of $B_{\Delta\square}$, $B_{\square\Delta} = B_{\Delta\square}^*$. When no ambiguity arise, we use the transpose matrix notation $B_{\square\Delta} = B_{\Delta\square}^\top$. For instance, $B_{XZ} = B_{ZX}^\top$, $B_{YC} = B_{CY}^\top$. Recall that the transformed input and output in Equation (16) and Equation (17) has the form

$$\psi_\gamma(X) = \psi(X) - E_X^p \phi(Z) + \sqrt{\gamma} E_X^p \phi(Z),$$

and

$$Y_\gamma = Y - E_Y^p \phi(Z) + \sqrt{\gamma} E_Y^p \phi(Z).$$

In the SEM case, the projections E_X^p and E_Y^p into $\phi(Z)$ are noted by the (composition of) operators in Equation (24) and Equation (25), where

$$E_X^p = (B_{XZ} + B_{XC}B_{CZ}),$$

and

$$E_Y^p = [B_{YZ} + B_{YC}B_{CZ} + B_{YX}(B_{XZ} + B_{XC}B_{CZ})].$$

As such, the transformed input and output has the form

$$\psi_\gamma(x) = B_{XC}\epsilon_C + \epsilon_X + \sqrt{\gamma}(B_{XZ} + B_{XC}B_{CZ})\phi(Z), \quad (26)$$

and

$$y_\gamma = (B_{YC} + B_{YX}B_{XC})\epsilon_C + B_{YX}\epsilon_X + \epsilon_Y + \gamma[B_{YZ} + B_{YC}B_{CZ} + B_{YX}(B_{XZ} + B_{XC}B_{CZ})]\phi(Z). \quad (27)$$

Define relevant covariance matrix/operators as $\Sigma_C = \mathbb{E}[\epsilon_C\epsilon_C^\top]$, $\Sigma_X = \mathbb{E}[\epsilon_X \otimes \epsilon_X]$ and $\Sigma_Z = \mathbb{E}[\phi(Z) \otimes \phi(Z)]$, where \otimes denotes the tensor outer product. Then the solution for the least square objective on the transformed input output can be written as

$$H^\gamma = \mathbb{E}[Y_\gamma\psi_\gamma(X)](\mathbb{E}[\psi_\gamma(X) \otimes \psi_\gamma(X)])^{-1}.$$

Plug in the transformed terms in the form of Equation (26) and Equation (27), we have

$$\begin{aligned} & \mathbb{E}[\psi_\gamma(X) \otimes \psi_\gamma(X)] \\ &= \mathbb{E}[(B_{XC}\epsilon_C + \epsilon_X + \sqrt{\gamma}(B_{XZ} + B_{XC}B_{CZ})\phi(Z))(B_{XC}\epsilon_C + \epsilon_X \\ & \quad + \sqrt{\gamma}(B_{XZ} + B_{XC}B_{CZ})\phi(Z))^\top] \\ &= B_{XC}\mathbb{E}[\epsilon_C\epsilon_C^\top]B_{CX} + \mathbb{E}[\epsilon_X \otimes \epsilon_X] \\ & \quad + \gamma(B_{XZ} + B_{XC}B_{CZ})\mathbb{E}[\phi(Z) \otimes \phi(Z)](B_{ZX} + B_{ZC}B_{CX}) \\ &= B_{XC}\Sigma_C B_{CX} + \Sigma_X + \gamma(B_{XZ} + B_{XC}B_{CZ})\Sigma_Z(B_{ZX} + B_{ZC}B_{CX}). \end{aligned}$$

Moreover, $\mathbb{E}[Y_\gamma\psi_\gamma(X)]$ has the form

$$\begin{aligned} & (B_{YC} + B_{YX}B_{XC})\mathbb{E}[\epsilon_C\epsilon_C^\top]B_{CX} + B_{YX}\mathbb{E}[\epsilon_X \otimes \epsilon_X] + \\ & \gamma[B_{YZ} + B_{YC}B_{CZ} + B_{YX}(B_{XZ} + B_{XC}B_{CZ})]\mathbb{E}[\phi(Z) \otimes \phi(Z)](B_{ZX} + B_{ZC}B_{CX}) \\ &= (B_{YC} + B_{YX}B_{XC})\Sigma_C B_{CX} + B_{YX}\Sigma_X + \\ & \gamma[B_{YZ} + B_{YC}B_{CZ} + B_{YX}(B_{XZ} + B_{XC}B_{CZ})]\Sigma_Z(B_{ZX} + B_{ZC}B_{CX}) \end{aligned}$$

as ϵ_C , ϵ_X and ϵ_Y are independent variables, which are also independent of Z . In overall, we have

$$\begin{aligned} H^\gamma &= [(B_{YC} + B_{YX}B_{XC})\Sigma_C B_{CX} + B_{YX}\Sigma_X \\ & \quad + \gamma[B_{YZ} + B_{YC}B_{CZ} + B_{YX}(B_{XZ} + B_{XC}B_{CZ})]\Sigma_Z(B_{ZX} + B_{ZC}B_{CX})] \\ & \quad [B_{XC}\Sigma_C B_{CX} + \Sigma_X + \gamma(B_{XZ} + B_{XC}B_{CZ})\Sigma_Z(B_{ZX} + B_{ZC}B_{CX})]^{-1} \end{aligned}$$

The bias of the target KAR estimator is then given by

$$\begin{aligned}
H^\gamma - B_{YX} &= \\
&\left[(B_{YC} + B_{YX}B_{XC})\Sigma_C B_{CX} + B_{YX}\Sigma_X \right. \\
&\quad \left. + \gamma[B_{YZ} + B_{YC}B_{CZ} + B_{YX}(B_{XZ} + B_{XC}B_{CZ})]\Sigma_Z(B_{ZX} + B_{ZC}B_{CX}) \right] \\
&\left[B_{XC}\Sigma_C B_{CX} + \Sigma_X + \gamma(B_{XZ} + B_{XC}B_{CZ})\Sigma_Z(B_{ZX} + B_{ZC}B_{CX}) \right]^{-1} - B_{YX} = \\
&\left[(B_{YC} + B_{YX}B_{XC})\Sigma_C B_{CX} + B_{YX}\Sigma_X \right. \\
&\quad \left. + \gamma[B_{YZ} + B_{YC}B_{CZ} + B_{YX}(B_{XZ} + B_{XC}B_{CZ})]\Sigma_Z(B_{ZX} + B_{ZC}B_{CX}) \right. \\
&\quad \left. - B_{YX}(B_{XC}\Sigma_C B_{CX} + \Sigma_X + \gamma(B_{XZ} + B_{XC}B_{CZ})\Sigma_Z(B_{ZX} + B_{ZC}B_{CX})) \right] \\
&\left[B_{XC}\Sigma_C B_{CX} + \Sigma_X + \gamma(B_{XZ} + B_{XC}B_{CZ})\Sigma_Z(B_{ZX} + B_{ZC}B_{CX}) \right]^{-1}
\end{aligned}$$

Collecting all the common terms we get

$$\begin{aligned}
H^\gamma - B_{YX} &= \left[\underbrace{B_{YC}\Sigma_C B_{CX}}_{\Sigma_{YX}^\perp} + \gamma \underbrace{(B_{YZ} + B_{YC}B_{CZ})\Sigma_Z(B_{ZX} + B_{ZC}B_{CX})}_{\Sigma_{YX}^\parallel} \right] \\
&\quad \left[B_{XC}\Sigma_C B_{CX} + \Sigma_X + \gamma(B_{XZ} + B_{XC}B_{CZ})\Sigma_Z(B_{ZX} + B_{ZC}B_{CX}) \right]^{-1}
\end{aligned}$$

Thus, $\forall x \in \mathcal{X}, y \in \mathcal{Y}$, consider the inner product $y^\top (H^\gamma - B_{YX})\psi(x) = 0$ when the following holds: (i) $B_{YC} = 0$ and $\gamma = 0$, or (ii) $B_{YZ} + B_{YC}B_{CZ} = 0$ and $\gamma = \infty$, or (iii) $B_{YC} = 0, B_{YZ} + B_{YC}B_{CZ} = 0$ and $\gamma \geq 0$, or (iv) $\Sigma_{YX}^\parallel = a\Sigma_{YX}^\perp$ for some $a > 0$, and $\gamma = \infty$, or (v) $\Sigma_{XY}^\parallel = -a\Sigma_{XY}^\perp$ for some $a > 0$, and $\gamma = 1/c$. As such, we conclude $H^\gamma = B_{XY}$. \square

A.3 Convergence rate for KAR.2 estimator

In this section, we will further discuss the convergence rate of **KAR.2** estimator, and show that the rate does not improve upon the convergence rate of **KAR** estimator.

In the three-stage KAR procedure, we approximate E_X^p and E_Y^p by $E_{\alpha_1, X}^{n_1}$ and $E_{\alpha_2, Y}^{n_2}$, respectively. In the two-stage KAR procedure, instead, we approximate the two operators by $E_{\alpha, X}^n$ and $E_{\alpha, Y}^n$, respectively. Note that the estimated operators $E_{\alpha, X}^n$ and $E_{\alpha, Y}^n$ use the same α . The shared α may fail to ensure the optimal approximation error for $E_{\alpha, X}^n$ and $E_{\alpha, Y}^n$ at the same time.

Lemma A12. Under Condition 1, $\forall \delta \in (0, 1)$, the following holds w.p. $1 - \delta$:

$$\|E_{\alpha, X}^n - E_X^p\|_{\mathcal{H}_\Gamma} \leq r_1(\alpha) := \frac{4\kappa(Q_1 + \kappa\|E_X^p\|_{\mathcal{H}_\Gamma}) \ln(2/\delta)}{\sqrt{n\alpha}} + \alpha^{\frac{c_1-1}{2}} \sqrt{\zeta_1}.$$

Under Condition 1 and Condition 2, $\forall \epsilon \in (0, 1)$, the following holds w.p. $1 - \epsilon$:

$$\|E_{\alpha, Y}^n - E_Y^p\|_{\mathcal{H}_\Theta} \leq r_2(\alpha) := \frac{4\kappa(Q_2 + \kappa\|E_Y^p\|_{\mathcal{H}_\Theta}) \ln(2/\epsilon)}{\sqrt{n}\alpha} + \alpha^{\frac{c_2-1}{2}} \sqrt{\zeta_2}.$$

Approximation error bound $r_1(\alpha)$ for $E_{\alpha, X}^n$ achieves its minimum at rate $O(n^{-\frac{c_1-1}{2(c_1+1)}})$ when

$$\alpha = \left(\frac{8\kappa(Q_1 + \kappa\|E_X^p\|_{\mathcal{H}_\Gamma}) \ln(2/\delta)}{\sqrt{n}\zeta_1(c_1 - 1)} \right)^{\frac{2}{c_1+1}} = O(n^{\frac{-1}{c_1+1}});$$

and approximation error bound $r_2(\alpha)$ for $E_{\alpha, Y}^n$ achieves its minimum at rate $O(n^{-\frac{c_2-1}{2(c_2+1)}})$ when

$$\alpha = \left(\frac{8\kappa(Q_2 + \kappa\|E_Y^p\|_{\mathcal{H}_\Theta}) \ln(2/\epsilon)}{\sqrt{n}\zeta_2(c_2 - 1)} \right)^{\frac{2}{c_2+1}} = O(n^{\frac{-1}{c_2+1}}).$$

Lemma A12 above provides the upper bounds of the approximation errors for $E_{\alpha, X}^n$ and $E_{\alpha, Y}^n$, and it's adapted from Theorem 2 in Singh et al. [2019]. We can see that if $c_1 \neq c_2$, we cannot claim the optimal convergence rate for $E_{\alpha, X}^n$ and $E_{\alpha, Y}^n$ at the same time, which disjoint sample sets projection estimators can guarantee by setting different α_1 and α_2 as shown in Lemma 1 and 2. In other words, in **KAR.2** procedure, the error propagated to the final stage, which are caused by using $E_{\alpha, X}^n$ and $E_{\alpha, Y}^n$, can have larger order than using $E_{\alpha_1, X}^{n_1}$ and $E_{\alpha_2, Y}^{n_2}$ separately in the **KAR** procedure. Therefore, we cannot ensure a same or improved convergence rate for **KAR.2** estimator compared to **KAR** estimator.

B Additional simulation details and results

B.1 Synthetic example in KIV setting

In this section, we show the data generating process and implementation details for the example used in the KIV [Singh et al., 2019] that follows the simulation case of learning counterfactual functions [Chen and Christensen, 2018] studied in Singh et al. [2019]. The structural model is set as follows,

$$Y = C + \ln(|16X - 8| + 1) \text{sgn}(X - 0.5).$$

The explanatory variables are generated from

$$\begin{pmatrix} C \\ V \\ W \end{pmatrix} \sim N \left(\begin{pmatrix} 0 \\ 0 \\ 0 \end{pmatrix}, \begin{pmatrix} 1, 0.5, 0 \\ 0.5, 1, 0 \\ 0, 0, 1 \end{pmatrix} \right),$$

$$X = F\left(\frac{W+V}{\sqrt{2}}\right),$$

$$Z = F(W),$$

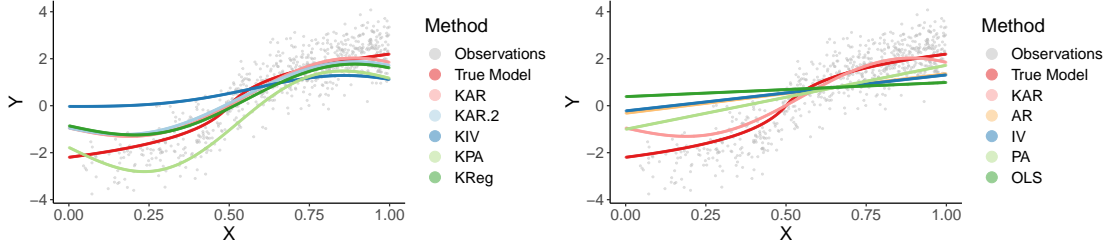


Figure B1: Variant synthetic example: fitted nonlinear (left) and linear (right) methods.

where F denote the c.d.f of standard normal distribution. This structural model ensures that anchor Z is a valid instrumental variable, so that KIV is supposed to perform well in this case. We conduct kernel anchor regression with three-stage algorithm (KAR), kernel anchor regression with two-stage algorithm (KAR.2) and multiple γ s and kernel instrument variable regression (KIV). Set $n_1 = 200$, $n_2 = 200$, $m = 600$, $n = n_1 + n_2 = 400$. For KAR and KAR.2, we set γ to be 0, 0.5, 1, 2, 5, 10, and 100. We set $\alpha_1 = c_\alpha n_1^{-0.5}$, $\alpha_2 = c_\alpha n_2^{-0.5}$, $\alpha = c_\alpha n^{-0.5}$, and $\xi = 1m^{-0.5}$, where $c_\alpha > 0$ is a constant chosen from $\{0.01, 0.05, 0.1, 0.5, 0.8, 1, 2, 3\}$ for each estimator separately to minimise the corresponding MSE. We use Gaussian kernel for all kernel methods, where the lengthscales are set according to median heuristic [Gretton et al., 2012].

For each algorithm, we then implement 50 simulations and calculate MSE with respect to the true causal model $\mathbb{E}(Y|do(x))$, which can be computed from the structural model. As shown in Figure 2(a), though KIV performs better than most KAR and KAR.2 estimators, KAR and KAR.2 with $\gamma = 2$ defeat KIV in the KIV setting. The parameters c_α s are chosen to be 1, 0.1, 3, 0.8, 3, 3, 3, 1, 0.1, 3, 1, 3, 3, 3 and 2 for KAR with γ being 0, 0.5, 1, 2, 5, 10, 100, KAR.2 with same γ series and KIV, respectively.

B.2 A variant of the synthetic data example

We also consider a variant case where the structural equation is same to the case in Section 5.1 in the main text

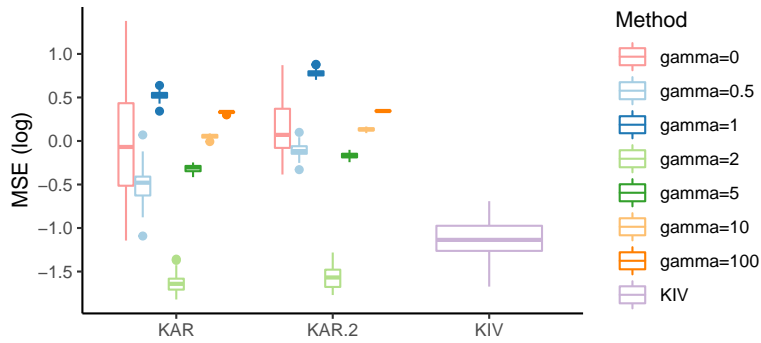
$$Y = 0.75C - 0.25Z + \ln(|16X - 8| + 1) \text{sgn}(X - 0.5),$$

and the explanatory variables are generated as

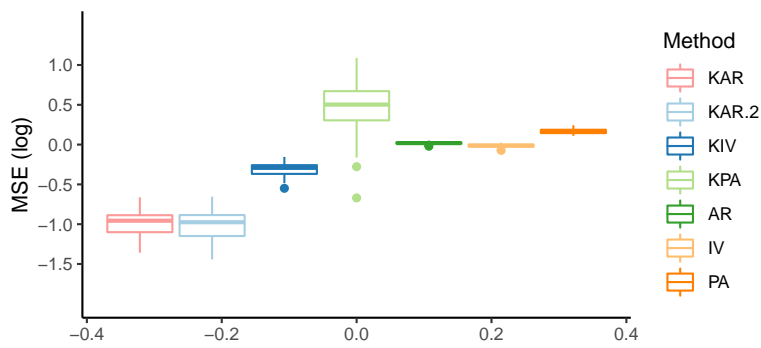
$$\begin{pmatrix} C \\ V \\ W \end{pmatrix} \sim N \left(\begin{pmatrix} 0 \\ 0 \\ 0 \end{pmatrix}, \begin{pmatrix} 1, 0.3, 0.2 \\ 0.3, 1, 0 \\ 0.2, 0, 1 \end{pmatrix} \right).$$

Instead, X and Z are set via the following transformation.

$$X = F \left(\frac{|W| + V}{\sqrt{2}} \right), \quad Z = F(|W|) - 0.5.$$



(a) MSE results in the KIV setting



(b) MSE results of all estimators in the variant case.

Figure B2: Experimental results for additional experiments.

The fitted result of nonlinear and linear methods is shown in Figure B1. The MSE averaged over 50 simulations is shown in Figure 2(b). From the result, we can also see that the proposed kernel anchor regression estimators still performs the best among others under the variant case.